A mathematical formalism for circulation in water mass configuration space

A. J. George Nurser[1,1], Stephen M. Griffies[2,2], Jan D. Zika[3,3], and Geoffrey J. Stanley[3,3]

[1]National Oceanography Centre
[2]NOAA Geophysical Fluid Dynamics Laboratory
[3]School of Mathematics and Statistics

November 30, 2022

Abstract

Projecting fluid systems onto coordinates defined by fluid properties (e.g., pressure, temperature, tracer concentration) can reveal deep insights, for example into the thermodynamics and energetics of the ocean and atmosphere. We present a mathematical formalism for fluid flow in such coordinates. We formulate mass conservation, streamfunction, tracer conservation, and tracer angular momentum within fluid property space (q-space) defined by an arbitrary number of continuous fluid properties. Points in geometric position space (x-space) do not generally correspond in a 1-to-1 manner to points in q-space. We therefore formulate q-space as a differentiable manifold, which allows differential and integral calculus but lacks a metric, thus requiring exterior algebra and exterior calculus. The Jacobian, as the ratio of volumes in x-space and q-space, is central to our theory. When x-space is not 1-to-1 with q-space, we define a generalized Jacobian either by patching x-space regions that are 1-to-1 with q-space, or by integrating a Dirac delta to select all x-space points corresponding to a given q value. The latter method discretises to a binning algorithm, providing a practical framework for analysis of fluid motion in arbitrary coordinates. Considering q-space defined by tracers, we show that tracer diffusion and tracer sources drive motion in q-space, analogously to how internal stresses and external forces drive motion in x-space. Just as the classical angular momentum of a body is unaffected by internal stresses, the globally integrated tracer angular momentum is unaffected by tracer diffusion — unless different tracers are diffused differently, as in double diffusion.

Mathematics of circulation in arbitrary fluid property spaces

A. J. George Nurser[1] †, Stephen M. Griffies[2,3], Jan D. Zika[4,5,6], and Geoffrey J. Stanley[4]

[1]National Oceanography Centre, University of Southampton Waterfront Campus, Southampton, UK

[2]NOAA Geophysical Fluid Dynamics Laboratory, Princeton, USA

[3]Princeton University Program in Atmospheric and Oceanic Sciences, Princeton, USA

[4]School of Mathematics and Statistics, University of New South Wales, Sydney, Australia

[5]UNSW Data Science Hub (uDaSH), University of New South Wales, Sydney, Australia

[6]Australian Centre for Excellence in Antarctic Science (ACEAS), University of New South Wales, Sydney, Australia

(Received xx; revised xx; accepted xx)

Projecting fluid systems onto coordinates defined by fluid properties (e.g., pressure, temperature, tracer concentration) can reveal deep insights, for example into the thermodynamics and energetics of the ocean and atmosphere. We present a mathematical formalism for fluid flow in such coordinates. We formulate mass conservation, streamfunction, tracer conservation, and tracer angular momentum within fluid property space ($\boldsymbol{q}$-space) defined by an arbitrary number of continuous fluid properties. Points in geometric position space ($\boldsymbol{x}$-space) do not generally correspond in a 1-to-1 manner to points in $\boldsymbol{q}$-space. We therefore formulate $\boldsymbol{q}$-space as a differentiable manifold, which allows differential and integral calculus but lacks a metric, thus requiring exterior algebra and exterior calculus. The Jacobian, as the ratio of volumes in $\boldsymbol{x}$-space and $\boldsymbol{q}$-space, is central to our theory. When $\boldsymbol{x}$-space is not 1-to-1 with $\boldsymbol{q}$-space, we define a generalized Jacobian either by patching $\boldsymbol{x}$-space regions that are 1-to-1 with $\boldsymbol{q}$-space, or by integrating a Dirac delta to select all $\boldsymbol{x}$-space points corresponding to a given $\boldsymbol{q}$ value. The latter method discretises to a binning algorithm, providing a practical framework for analysis of fluid motion in arbitrary coordinates. Considering $\boldsymbol{q}$-space defined by tracers, we show that tracer diffusion and tracer sources drive motion in $\boldsymbol{q}$-space, analogously to how internal stresses and external forces drive motion in $\boldsymbol{x}$-space. Just as the classical angular momentum of a body is unaffected by internal stresses, the globally integrated tracer angular momentum is unaffected by tracer diffusion — unless different tracers are diffused differently, as in double diffusion.

1. Introduction

The review paper from Groeskamp *et al.* (2019) proposed that ocean circulation described in terms of the kinematics of water mass space complements the traditional Eulerian and Lagrangian kinematics (both referred to as $\boldsymbol{x}$-space). We here further this proposition by

† Email address for correspondence: g.nurser@noc.ac.uk

establishing a mathematical formalism for describing circulation in the space defined by continuous fluid properties (here abbreviated as $\boldsymbol{q}$-space). In so doing we expose coordinate-invariant elements of the $\boldsymbol{q}$-space circulation and reveal novel insights available when choosing specific coordinates, thus fostering physical understanding.

Our goal is to provide a mathematical foundation to support novel analyses of the circulation of a fluid dynamical system with an arbitrary number of continuously varying properties. We are primarily motivated by the many oceanographic applications of circulation in water mass spaces. There are also direct applications of this perspective to the study of atmospheric circulations as viewed in the corresponding air mass space. The studies from Pauluis & Held (2002), Kjellsson *et al.* (2014), Laliberté *et al.* (2015), and Döös *et al.* (2017) provide examples. We generalise this discussion to what one might call an analysis in fluid property space, and we do so by formulating fluid flow in an arbitrary space defined by continuous coordinates.

1.1. *From water mass space to fluid property space*

Water mass analysis—as introduced by Walin (1977, 1982) and extended by Speer & Tziperman (1992), Nurser *et al.* (1999), Marshall *et al.* (1999), Iudicone *et al.* (2008) (see Groeskamp *et al.* (2019) for more references)—is concerned with seawater motion within and across layers defined by a single continuous property, typically a tracer concentration or buoyancy. It therefore involves a 1-D $\boldsymbol{q}$-space, though this is sometimes extended with one geographical coordinate into a mixed 2-D $\boldsymbol{q}$-space, such as defined by buoyancy b and latitude ϕ, or by temperature and latitude (Holmes *et al.* 2019). Isopycnal ocean models are couched in terms of a mixed 3-D $\boldsymbol{q}$-space involving buoyancy, latitude, and longitude, while Winters & D'Asaro (1996) used a mixed 3-D $\boldsymbol{q}$-space involving an arbitrary scalar, along with horizontal position (x, y) to study the increased mixing associated with folded and broken-up surfaces of constant scalar. Extension to a 2-D $\boldsymbol{q}$-space involving the two active tracers Conservative Temperature, Θ, and salinity, S, has illuminated our view of the oceanic thermohaline circulation (Speer 1993; Zika *et al.* 2012; Döös *et al.* 2012; Hieronymus *et al.* 2014; Groeskamp *et al.* 2014), providing images of the ocean circulation such as in Figure 1.

Water mass analysis is concerned with the hows and whys of seawater movement across coordinate surfaces. If those surfaces are defined by tracers or buoyancy, as is traditional, then cross-surface motion is caused by irreversible processes such as mixing, radiant heating, and turbulent boundary fluxes; the associated water mass analysis naturally disregards reversible processes while focusing on irreversible processes. In the oceanic context, there are many possible water mass spaces, defined by a variety of measured ocean properties, including material tracer concentrations (salinity, carbon, chemical tracers, biogeochemical tracers), dynamical tracers (potential vorticity), thermo-mechanical properties (Conservative Temperature, pressure), and buoyancy (potential density, neutral density). We here generalise the mathematical formalism of water mass analysis with the aim to facilitate the study of fluid circulation within a wide variety of possible fluid property spaces.

Our formulation is partly inspired by the treatment of thermodynamics in Section 5.1 of Schutz (1980) and Section 6.3 of Frankel (2012). Their approach conceives of an equilibrium thermodynamic system as living at a point within a thermodynamic configuration space, which is generally a smooth manifold on which the rules of differential and integral calculus hold, and quasi-static processes lead to continuous movement or trajectories on this manifold. Thermodynamic configuration space is not endowed with a metric, but smoothness ensures that it satisfies the properties of a differentiable manifold (e.g. Chapter 1 of Frankel 2012). The absence of a metric represents a key mathematical distinction from the Euclidean space of Newtonian mechanics, as Euclidean space is endowed with the Kronecker metric. Without a metric, we cannot measure distance or angles. However, we can still derive differential and

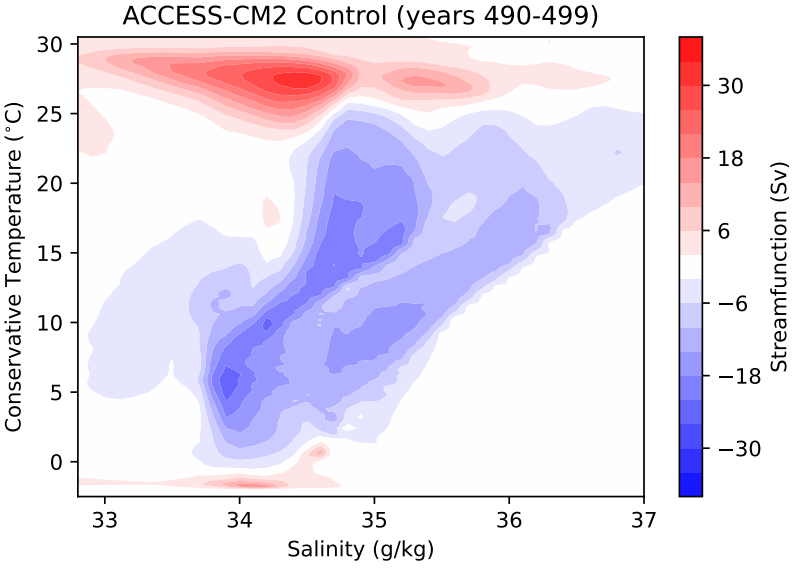

Figure 1: Global ocean circulation (units of Sv = 10^9 kg s^{-1}) as represented in the water mass space of preformed salinity and Conservative Temperature: $(q^1, q^2) = (S, \Theta)$. The transport is computed from results generated by the ACCESS-CM2 climate model (Bi *et al.* 2020) run under pre-industrial radiative forcing, and using model years 1440-1449 (years 490-499 of the piControl). Blue (negative) circulation is clockwise and red (positive) is counter-clockwise. See Zika *et al.* (2012), Döös *et al.* (2012), Hieronymus *et al.* (2014), and Groeskamp *et al.* (2014) for discussions of the physics of this circulation.

integral budgets by using rudimentary features of exterior forms (also known as differential forms; see Appendix B). In essence, this paper replaces "thermodynamic configuration space" with "fluid property space" and develops the mathematical physics of this space for non-equilibrium fluid systems.

1.2. *Limitations of fluid property space*

As in thermodynamics, our formulation is not based on assuming a 1-to-1 invertible relation between $\boldsymbol{q}$-space and $\boldsymbol{x}$-space. Rather, our fundamental assumption is that fluid property space is a smooth and orientable differentiable manifold, thus enabling the use of calculus. (Note that a manifold is orientable if we can define handedness continuously over the manifold; i.e., there is a consistent definition of clockwise and counter-clockwise. For example, Euclidean space is orientable whereas a Möbius strip is not.) Starting from this minimalist position allows us to develop a general theory that then offers avenues for specialization.

How common is the lack of a global 1-to-1 mapping from $\boldsymbol{x}$-space to $\boldsymbol{q}$-space? The answer depends on specifics of the fluid property coordinates. For example, if $\boldsymbol{q}$-space has fewer than three dimensions then there is no continuous function that can map $\boldsymbol{x}$-space 1-to-1 to $\boldsymbol{q}$-space. Even if $\boldsymbol{q}$-space is three-dimensional, a 1-to-1 mapping is not guaranteed. Consider, as Zika *et al.* (2013) did, analysing the ocean in thermodynamic coordinates, with $\boldsymbol{q} = (S, \Theta, p)$ defined by Absolute Salinity, Conservative Temperature, and pressure. In this case, a curve of constant (S, Θ) will often have multiple points with the same pressure (Figure 2), and thus the mapping from $\boldsymbol{x}$-space to $\boldsymbol{q}$-space is not globally 1-to-1. As a further example, consider small scale turbulent flows where surfaces of constant property are commonly broken up into discontinuous blobs. For such flows, a global 1-to-1 mapping cannot be expected.

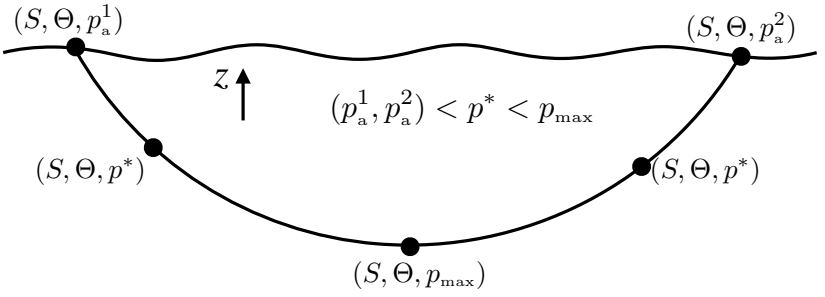

Figure 2: Illustrating with $\boldsymbol{q} = (S, \Theta, p)$ that the mapping from $\boldsymbol{x}$-space to $\boldsymbol{q}$-space is, generally, not 1-to-1. Here we show a curve of constant (S, Θ), formed by the intersection of a constant S surface and constant Θ surface. This (S, Θ)-curve outcrops at two points on the ocean surface where the atmospheric pressure is p_a^1 and p_a^2. Somewhere along the curve there are at least two points with pressure, $p = p^*$, that is less than the maximum pressure along the curve, $p^* < p_{max}$, yet greater than either atmospheric pressures, $(p_a^1, p_a^2) < p^*$. Hence, there are at least two points along the (S, Θ)-curve with the same value for $\boldsymbol{q}$ but distinct values for $\boldsymbol{x}$.

We pay a price when working in a fluid property space that does not have a global 1-to-1 mapping from $\boldsymbol{x}$-space. Namely, $\boldsymbol{q}$-space is not generally suited for examining dynamical effects associated with the contact stresses from pressure and friction. The reason is that contact stresses occur between fluid elements that are adjacent in $\boldsymbol{x}$-space, and such locality is lost if the mapping from $\boldsymbol{x}$-space to $\boldsymbol{q}$-space is not 1-to-1. Now, there are physically interesting cases where $\boldsymbol{q}$-space *does* have a 1-to-1 mapping from $\boldsymbol{x}$-space, either globally or locally. For example, Salmon (2013) considered a $\boldsymbol{q}$-space comprised of three tracer-like coordinates that retain a 1-to-1 mapping from $\boldsymbol{x}$-space. Even so, we are not focused on the study of fluid dynamics (i.e., Newton's second or third laws) in $\boldsymbol{q}$-space. Rather, we pursue the traditional approach of water/air mass analysis by examining fluid circulation, mass, and tracer budgets in $\boldsymbol{q}$-space.

1.3. *Content of this paper*

We start, in Section 2, by presenting the basic elements of fluid property space. We here encounter the central role played by the mass density function, $\mathfrak{m}$, which provides a measure of the mass per unit $\boldsymbol{q}$-space volume. In Section 3, we describe how to relate $\boldsymbol{x}$-space and $\boldsymbol{q}$-space whether or not the mapping between these spaces is 1-to-1. Our method allows for a unified treatment of differential budgets derived in subsequent sections. We then provide a $\boldsymbol{q}$-space derivation of mass conservation in Section 4. Although seemingly quite trivial, the resulting conservation equation (**??**) is fully general and thus provides a measure for mass balances in $\boldsymbol{q}$-space for any number of arbitrary coordinates. We also consider the special case of steady circulation in the absence of mass sources, which affords a $\boldsymbol{q}$-space mass transport streamfunction. In Section 5, we introduce the $\boldsymbol{q}$-space angular momentum and derive local and global properties. We find that the $\boldsymbol{q}$-space angular momentum offers a more versatile means to characterize $\boldsymbol{q}$-space circulation than the streamfunction. In Section 6, we extend the derivation of mass conservation to yield an equation for tracer conservation (the tracer equation). We then apply the formalism in Section **??** to the special case of fluid property space defined by tracer coordinates, in which case we directly connect motion in tracer space to mixing and other irreversible processes. Remarkably, we show that globally integrated properties of the tracer space angular momentum and steady circulation are unaffected by diffusion. We close the main part of the paper in Section 8 with summary and conclusions.

Appendix A provides a few examples for the Laplace operator used for subgrid scale

tracer diffusion. In traditional treatments this operator is derived using covariant derivatives, which require a metric tensor. However, our metric-free approach using exterior forms only makes use of partial derivatives. Appendix B rounds out the paper with a tutorial on exterior (or differential) forms. Both the mathematically experienced reader and the mathematically trusting reader will find Appendix B unnecessary for the main text. Even so, it is offered for the curious reader who wishes to better understand the mathematical concepts in the main text. As this paper contains many mathematical symbols, we present Table 1 to summarize frequently used symbols.

2. Elementary aspects of fluid property space

We refer to the geometric position space as $\boldsymbol{x}$-space and write its coordinates as

$$\boldsymbol{x} = (x^1, x^2, x^3) = x^a. \tag{2.1}$$

Labels $a = 1, 2, 3$ distinguish the coordinate components rather than indicate a power. Within a continuum description of fluids, each infinitesimal fluid element has a unique value for the position coordinate, $\boldsymbol{x}$.

We organize the continuous-valued fluid properties into an array

$$\boldsymbol{q} = (q^1, q^2, q^3, \ldots q^N) = q^\alpha, \tag{2.2}$$

with $N \geqslant 1$ the number of properties. The properties, q^α, define coordinates for a point within fluid property space ($\boldsymbol{q}$-space), with the number of properties, N, determining the dimension of $\boldsymbol{q}$-space. The Greek superscripts signify a particular property rather than denoting a power, and with Greek labels used for $\boldsymbol{q}$-space coordinates as distinguished from the Latin labels used for $\boldsymbol{x}$-space coordinates. Depending on the fluid system and the chosen $\boldsymbol{q}$-space, each point in $\boldsymbol{q}$-space may or may not correspond to a unique point in $\boldsymbol{x}$-space.

2.1. *Assumptions about $\boldsymbol{q}$-space*

Our mathematical formulation allows fluid property space to be defined by an arbitrary number of coordinates, with examples for $N = 1, 2, 3$ offered to touch base with common applications. Furthermore, $\boldsymbol{q}$-space can be built from any continuous property, including coordinates from $\boldsymbol{x}$-space.

2.1.1. *$\boldsymbol{q}$-space defines a differentiable manifold*

We assume that the continuous coordinates of $\boldsymbol{q}$-space define a smooth and orientable differentiable manifold. Doing so allows us to use differential and integral calculus to study mass budgets and circulation in $\boldsymbol{q}$-space. Under these assumptions, fluid property space locally resembles Euclidean space, with differentiation and integration carried from Euclidean space to $\boldsymbol{q}$-space. Hence, differential conservation laws in $\boldsymbol{q}$-space have expressions reminiscent of Cartesian coordinates, and integrals over this manifold take their familiar form. However, there is generally no metric structure in $\boldsymbol{q}$-space. Consequently, we cannot always access familiar tools from vector calculus and tensor analysis, such as distance, angles, outward normal vectors, inner products, covariant derivatives, and curvature.

2.1.2. *Use of the exterior product for orientation*

For budget analyses in $\boldsymbol{x}$-space we generally rely on outward normal vectors to orient surfaces, volumes, and transport. However, the absence of a metric for $\boldsymbol{q}$-space affords it a rather minimalist mathematical structure thus necessitating an alternative means for orientation. For that purpose, we orient surfaces and surface elements within $\boldsymbol{q}$-space through the anti-symmetry property of the exterior product, which we introduce in Section 2.3 and further

Table 1: Table summarizing the key symbols used in this paper.

SYMBOL	MEANING
$\boldsymbol{x}, x^a$	coordinates for physical space
a, b, c	$\boldsymbol{x}$-space coordinate labels
$\boldsymbol{q}, q^\alpha$	coordinates for fluid property space; $\alpha \in \{1, 2, \ldots, N\}$
N	number of dimensions for $\boldsymbol{q}$-space
α, β, γ	$\boldsymbol{q}$-space coordinate labels
$\dot{\boldsymbol{x}}, \dot{x}^a$	velocity in $\boldsymbol{x}$-space and its components
$\dot{\boldsymbol{q}}, \dot{q}^\alpha$	velocity in $\boldsymbol{q}$-space and its components
$\mathcal{X}$	ocean domain in $\boldsymbol{x}$-space
$\mathfrak{q}$	function measuring $\boldsymbol{q}$ at $\boldsymbol{x} \in \mathcal{X}$
$\dot{\mathfrak{q}}$	function measuring $\dot{\boldsymbol{q}}$ at $\boldsymbol{x} \in \mathcal{X}$
$\mathfrak{q}(\mathcal{X})$	$\boldsymbol{q}$-space image of the ocean domain
$\mathcal{Q}$	subset of $\boldsymbol{q}$-space; codomain of $\mathfrak{q}$
$\partial_a = \partial/\partial x^a$	$\boldsymbol{x}$-space partial derivative
$\partial_\alpha = \partial/\partial q^\alpha$	$\boldsymbol{q}$-space partial derivative
d	exterior derivative operator
$\wedge$	exterior (or wedge) product
$\mathrm{d}V$	$\boldsymbol{x}$-space volume element
$\mathrm{d}\mathcal{V}$	$\boldsymbol{q}$-space volume element
ρ	mass per volume in $\boldsymbol{x}$-space
$\mathfrak{m}$	mass per volume in $\boldsymbol{q}$-space
$\mathrm{d}M$	mass of an elementary ocean region
$\mathcal{J}$	Jacobian from $\boldsymbol{q}$-space to $\boldsymbol{x}$-space
$\mathcal{G}$	inverse Jacobian from $\boldsymbol{x}$-space to $\boldsymbol{q}$-space
$\mathcal{T}$	mass transport exterior form (mass per time)
$\mathcal{M}$	mass source (mass per time)
ψ, ψ_α	steady mass transport streamfunctions
$\epsilon^{\alpha\beta} = \epsilon_{\alpha\beta}$	permutation symbol for $\boldsymbol{q}$-space with $N = 2$
$\epsilon^{\alpha\beta\gamma} = \epsilon_{\alpha\beta\gamma}$	permutation symbol for $\boldsymbol{q}$-space with $N = 3$
$\Pi_{\tilde{\boldsymbol{q}}}(\boldsymbol{q})$	Dimensionless boxcar (binning) function
$\delta_{\tilde{\boldsymbol{q}}}(\boldsymbol{q})$	Dirac delta for $\boldsymbol{q}$-space with dimensions $\mathcal{V}^{-1}$
$\delta^\alpha_\beta = \delta_{\alpha\beta}$	Kronecker symbol = unit tensor
$I \in \{1, \ldots, N_{\mathrm{P}}\}$	label for N_{P} coordinate patches
$\boldsymbol{C}, C^\alpha$	tracer concentrations
$\mathcal{T}_C$	tracer transport exterior form
$\rho\, \boldsymbol{F}, \rho\, F^a$	$\boldsymbol{x}$-space subgrid tracer flux
$\mathfrak{m}\, F^\alpha$	$\boldsymbol{q}$-space subgrid tracer flux
$\boldsymbol{K}, \mathbb{K}$	symmetric diffusivity tensor
$\mathcal{S}$	combined tracer source
S	Absolute Salinity
Θ	Conservative Temperature
p	pressure
b	buoyancy
ϕ	latitude
$\mathcal{D}$	subgrid tracer operator

detail in Appendix B. Doing so allows us to determine whether a transport adds or removes matter from a $\boldsymbol{q}$-space region, thus facilitating the development of budget equations.

2.1.3. *Emphasizing a property of partial derivatives*

We only use partial derivatives throughout this paper; covariant derivatives are not used since they require a metric tensor. When performing partial derivatives, we emphasize that all other coordinates are held fixed. For example, the $\boldsymbol{x}$-space partial derivative,

$$\partial_a = \frac{\partial}{\partial x^a} \tag{2.3}$$

is computed by holding all other coordinates, x^b where $b \neq a$, fixed. In this manner,

$$\partial_a x^b = \delta_a^b \quad \text{and} \quad \partial_a x^a = 3, \tag{2.4}$$

with δ_a^b the components to the Kronecker or identity tensor, and the second equality made use of the summation convention where repeated indices are summed over their range. The same identities hold when performing derivatives in $\boldsymbol{q}$-space, so that

$$\partial_\alpha = \frac{\partial}{\partial q^\alpha} \quad \text{and} \quad \partial_\alpha q^\beta = \delta_\alpha^\beta \quad \text{and} \quad \partial_\alpha q^\alpha = N. \tag{2.5}$$

These identities are central to many of the manipulations in this paper.

2.2. *Mass and mass density in $\boldsymbol{q}$-space*

We make use of the mass density function, $\mathfrak{m}(\boldsymbol{q}, t)$, that measures the fluid mass, $\mathrm{d}M$, within an elemental $\boldsymbol{q}$-space volume, $\mathrm{d}\mathcal{V}$,

$$\mathrm{d}M = \mathfrak{m}\, \mathrm{d}\mathcal{V}. \tag{2.6}$$

In Figure 3 we illustrate the case of $N = 1$ with $q^1 = \Theta$, whereby the ocean is binned according to Conservative Temperature classes. At any time instance, the density function, $\mathfrak{m}(\Theta, t)$, allows us to compute the mass of fluid, $\mathrm{d}M = \mathfrak{m}\, \mathrm{d}\Theta$, that is contained within a Conservative Temperature bin, $[\Theta - \Delta\Theta/2, \Theta + \Delta\Theta/2)$, in the limit as the bin size becomes infinitesimal, $\Delta\Theta \to \mathrm{d}\Theta$. In Figure 4 we extend the fluid property space dimension to $N = 2$ by displaying the mass density function for $\boldsymbol{q} = (S, \Theta)$.

2.3. *Volume elements in $\boldsymbol{q}$-space*

The volume element, $\mathrm{d}\mathcal{V}$, measures the coordinate volume of an elementary region of $\boldsymbol{q}$-space. For example, with $N = 1$ we have the volume element given by

$$\mathrm{d}\mathcal{V} = \mathrm{d}q^1, \tag{2.7}$$

such as the case with $q^1 = \Theta$ discussed above whereby $\mathrm{d}\mathcal{V} = \mathrm{d}\Theta$. When $N > 1$, we write the volume element as an exterior N-form (N-form for brief),

$$\mathrm{d}\mathcal{V} \equiv \mathrm{d}q^1 \wedge \mathrm{d}q^2 \wedge \ldots \mathrm{d}q^N, \tag{2.8}$$

with $\wedge$ the exterior (or wedge) product. For example, with $N = 3$ and $\boldsymbol{q} = (S, \Theta, p)$, the volume 3-form in $\boldsymbol{q}$-space is

$$\mathrm{d}\mathcal{V} = \mathrm{d}S \wedge \mathrm{d}\Theta \wedge \mathrm{d}p. \tag{2.9}$$

Similarly, for $N = 2$ with $\boldsymbol{q} = (S, \Theta)$, the volume 2-form is

$$\mathrm{d}\mathcal{V} = \mathrm{d}S \wedge \mathrm{d}\Theta. \tag{2.10}$$

In Figure 5 we depict a Cartesian area element 2-form, $\mathrm{d}y \wedge \mathrm{d}z$.

The exterior product is anti-symmetric so that odd permutations of differentials lead to a sign change whereas even permutations retain the sign. For example,

$$\mathrm{d}\mathcal{V} = \mathrm{d}S \wedge \mathrm{d}\Theta \wedge \mathrm{d}p = -\mathrm{d}\Theta \wedge \mathrm{d}S \wedge \mathrm{d}p = \mathrm{d}p \wedge \mathrm{d}S \wedge \mathrm{d}\Theta. \tag{2.11}$$

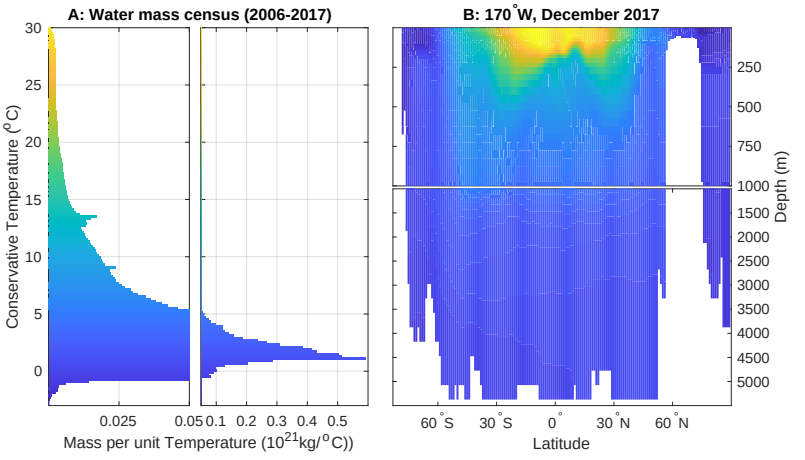

Figure 3: Left panel (A): mass density function, $\mathfrak{m}(\Theta)$, for a one-dimensional ($N = 1$) fluid property space defined by Conservative Temperature, $q^1 = \Theta$, as time averaged over years 2006-2017. The density function has units of 10^{21} kg/°C. Note the split in the horizontal (mass density) axis, thus enabling a more refined view of the density function in the less populated warm and cold waters. Right panel (B): a meridional section at 170°W for December 2017, thus providing a sample of the spatial distribution of Θ. The split in the vertical axis enables a more refined view of the upper ocean warm and cold waters. We use observational based data for the World Ocean as estimated by the objective analysis from the Enact Ensemble (V4.0; Good *et al.* (2013)).

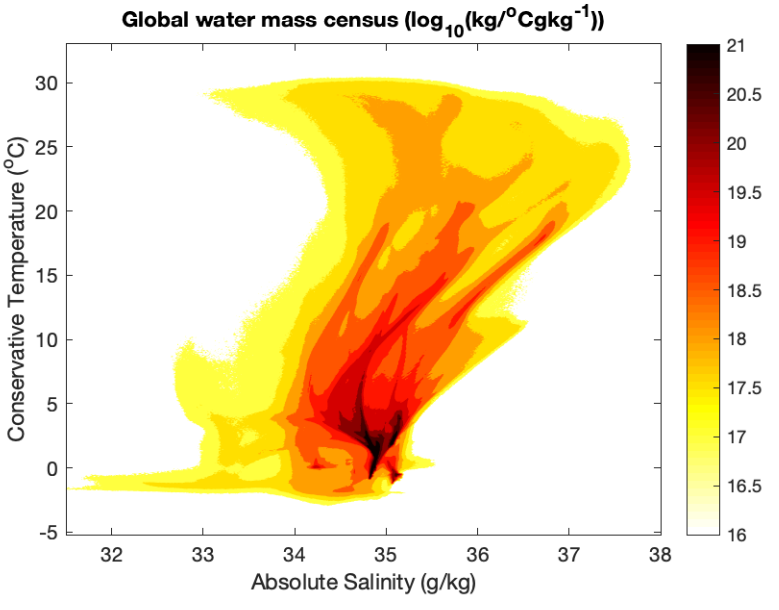

Figure 4: The log of a mass density function, $\mathfrak{m}(S, \Theta)$ averaged over years 2006-2017 for a two-dimensional ($N = 2$) fluid property space defined by Absolute Salinity, S, and Conservative Temperature, Θ, so that $(q^1, q^2) = (S, \Theta)$. The density function has units of kg/[°C (g/kg)]. We use observational based data for the World Ocean as estimated by the objective analysis from the Enact Ensemble (V4.0; Good *et al.* (2013)). See Zika *et al.* (2021) for more discussion of this distribution and its changes arising from climate warming.

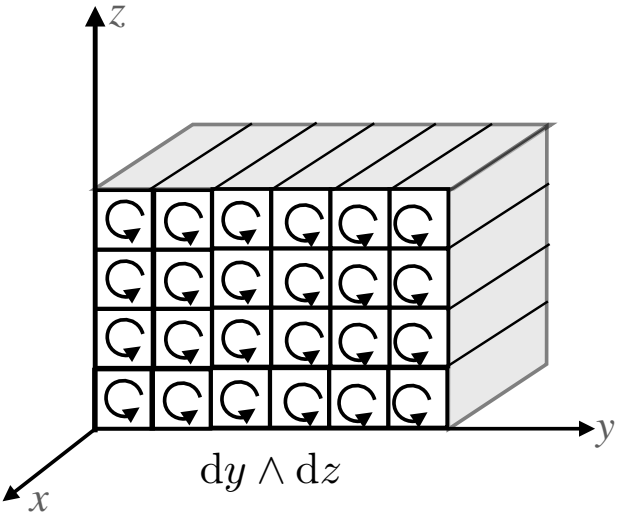

Figure 5: Schematic of the area 2-form, $\mathrm{d}y \wedge \mathrm{d}z$. For Euclidean space we can establish a geometric interpretation of the 1-form $\mathrm{d}y$ as an infinite sequence of horizontal planes perpendicular to the y-axis. Likewise, the 1-form $\mathrm{d}z$ defines surfaces perpendicular to the z-axis. The exterior product $\mathrm{d}y \wedge \mathrm{d}z$ is the intersection of these surfaces that produces an infinite lattice of infinitesimal oriented cells. By convention, we associate counter-clockwise swirls in each of the infinitesimal cells of area $\mathrm{d}y \wedge \mathrm{d}z$ as a means to orient the area elements according to the right hand rule. This image is adapted from Figure 4.1 of Misner *et al.* (1973).

Hence, the exterior volume form, $\mathrm{d}\mathcal{V}$, is not sign-definite.

3. How to relate $\boldsymbol{x}$-space and $\boldsymbol{q}$-space

In this Section we detail how to relate $\boldsymbol{x}$-space and $\boldsymbol{q}$-space. We start in Section 3.1 by discussing the basic functional properties of the function, $\mathfrak{q}$, that maps from $\boldsymbol{x}$-space to $\boldsymbol{q}$-space. After discussing trajectories in $\boldsymbol{q}$-space in Section 3.2, we use these functional properties to split the theory for mapping from physical space to fluid property space into two cases. Section 3.3 considers the first case, in which $N = 3$ and $\mathfrak{q}$ is a bijection between $\boldsymbol{x}$-space and $\boldsymbol{q}$-space. This case enables the use of coordinate transformation formulas from elementary calculus and tensor analysis. We then generalize in Section 3.4 to the case where $\mathfrak{q}$ is not a bijection.

3.1. *Characterizing mappings between $\boldsymbol{x}$-space and $\boldsymbol{q}$-space*

Let $\mathcal{X}$ be a subset of $\boldsymbol{x}$-space that could represent the entire fluid domain or a subset. Note that $\mathcal{X}$ could be time-dependent. Measuring fluid properties at points in the domain, $\boldsymbol{x} \in \mathcal{X}$, and times t determines values for the function $\mathfrak{q}(\boldsymbol{x}, t)$. We assume throughout this paper that $\mathfrak{q}$ is a continuously differentiable function. For brevity, we often treat the time-dependence implicitly; that is, for a fixed time t we simply write $\mathfrak{q}(\boldsymbol{x})$ and treat $\mathfrak{q}$ as a function from domain $\mathcal{X}$ to codomain $\mathcal{Q}$, where $\mathcal{Q}$ is generally a subset of $\boldsymbol{q}$-space. This shorthand applies for the rest of this subsection, in which we restrict attention to a fixed but arbitrary time, t.

In Case 1, let $N = 3$ and suppose that $\mathfrak{q}$ is a *bijection* from $\mathcal{X}$ to $\mathcal{Q}$. This case is equivalent to supposing that $\mathfrak{q}$ is both a *1-to-1* function (also called an *injection*) and an *onto* function (also called a *surjection*). To be 1-to-1 means that $\mathfrak{q}$ maps distinct points in $\mathcal{X}$ to distinct points in $\mathcal{Q}$. That is, if $\boldsymbol{x}_1 \neq \boldsymbol{x}_2$ are two distinct points both in $\mathcal{X}$, then $\mathfrak{q}(\boldsymbol{x}_1) \neq \mathfrak{q}(\boldsymbol{x}_2)$ are two

distinct points both in $\mathcal{Q}$. To be onto means that $\mathfrak{q}$ reaches every point in $\mathcal{Q}$; that is, for every $\boldsymbol{q} \in \mathcal{Q}$ there is some $\boldsymbol{x} \in \mathcal{X}$ such that $\mathfrak{q}(\boldsymbol{x}) = \boldsymbol{q}$. Case 1 is depicted in the top panel of Figure 6. As a bijection, the function $\mathfrak{q}$ has an inverse function, denoted $\mathfrak{q}^{-1}$, that is a bijection that maps from $\mathcal{Q}$ to $\mathcal{X}$. As such, no information is lost when using $\mathfrak{q}$ to map between $\mathcal{X}$ and $\mathcal{Q}$.

In Case 2, $\mathfrak{q}$ is not 1-to-1, and may or may not be onto, as depicted in the bottom panel of Figure 6. For $\mathfrak{q}$ to not be 1-to-1 (also called many-to-1) implies that there are distinct points in $\mathcal{X}$ that map to the same point in $\mathcal{Q}$. We introduced the many-to-1 mapping case in Section 1.2. As another example, $\mathfrak{q}$ is many-to-1 if there are regions of finite volume in $\boldsymbol{x}$-space where some or all of the properties, q^α, are homogeneous. Such many-to-1 mappings are not invertible bijections so that information is lost in the process of mapping. While $\mathfrak{q}$ may or may not be many-to-1 for $N \geqslant 3$, when $N < 3$ it is guaranteed that $\mathfrak{q}$ is many-to-1 (having assumed $\mathfrak{q}$ is continuous). For example, with $\boldsymbol{q} = (b, \phi)$ defined by buoyancy and latitude, the zonal direction is integrated out so there is no information about zonal position. Likewise, mapping the ocean to either $\boldsymbol{q} = (S, \Theta)$ or $q = \Theta$ reduces the dimensionality of $\boldsymbol{q}$-space relative to the three dimensions of $\boldsymbol{x}$-space.

The most important distinction between the above two Cases is whether $\mathfrak{q}$ is 1-to-1 or not. If $\mathfrak{q}$ is 1-to-1, we can define the codomain $\mathcal{Q}$ to be the image of $\mathfrak{q}$, denoted $\mathfrak{q}(\mathcal{X})$. While $\mathfrak{q}(\mathcal{X})$ will be time-dependent and may have non-trivial geometric and topological properties, this choice means $\mathfrak{q}$ is onto, by definition, which further implies that $\mathfrak{q}$ is a bijection, placing us into Case 1. In Case 2, $\mathfrak{q}$ being many-to-1 implies $\mathfrak{q}$ is not a bijection. Having already lost this desirable property, we care less about whether $\mathfrak{q}$ is onto (surjective).

The upside of Case 2 is that we can define $\mathcal{Q}$ as a larger space than just the set of $\boldsymbol{q}$ values found in the ocean, $\mathfrak{q}(\mathcal{X})$. Most simply, we may define $\mathcal{Q}$ as all of $\boldsymbol{q}$-space, which is the Cartesian product of the valid ranges for each fluid property q^α. For $\boldsymbol{q}$-space coordinates that are specified by a material tracer concentration, then the physical value of the coordinate can range between zero and unity, even if the maximum tracer concentration anywhere in the fluid domain is a small fraction of unity. Similarly, the range for temperature, in the oceanic case, can be extended beyond the values for which seawater is liquid (which depends on pressure and salinity and would thus be time-dependent), to any value above -273.15°C. For example, if $\boldsymbol{q} = (S, \Theta)$ with S measured in g kg^{-1} and Θ in °C, then $\boldsymbol{q}$-space is $[0, 1000] \times [-273.15, \infty)$. We will see that this extension of $\boldsymbol{q}$-space causes no problems, as the functions used in our fluid property space theory are simply zero outside $\mathfrak{q}(\mathcal{X})$.

In practical calculations, the mapping $\mathfrak{q}$ from $\boldsymbol{x}$-space to $\boldsymbol{q}$-space is discretely realized via a binning algorithm (e.g., Section 7.5 of Groeskamp *et al.* 2019), with the continuous formulation of this paper recovered by letting the bin size be infinitesimal.

3.2. *Trajectories and velocity in $\boldsymbol{x}$-space and $\boldsymbol{q}$-space*

We here consider motion in $\boldsymbol{q}$-space and how it is related to motion in $\boldsymbol{x}$-space. Notably, motion in $\boldsymbol{x}$-space may correspond to no motion in $\boldsymbol{q}$-space, for example when $\boldsymbol{q} = (S, \Theta)$ and a fluid element in $\boldsymbol{x}$-space experiences only adiabatic and isohaline physical processes (e.g., linear waves or laminar advection). Likewise, motion in $\boldsymbol{q}$-space could correspond to no motion in $\boldsymbol{x}$-space, for example when $\boldsymbol{q} = (S, \Theta)$ and a region of the ocean is at rest but experiences uniform radiative forcing or uniform diabatic mixing.

The trajectory of a fluid particle in $\boldsymbol{x}$-space, having initial position $\boldsymbol{x}_0$ at time t_0, is described by a function $\boldsymbol{X}(t)$ that satisfies $\boldsymbol{X}(t_0) = \boldsymbol{x}_0$ (e.g., Salmon 1998; van Sebille *et al.* 2018). To determine $\boldsymbol{X}$ requires knowing the velocity, $\dot{\boldsymbol{x}} = \boldsymbol{v}(\boldsymbol{x}, t)$, which in a continuum fluid is a continuous space-time field. Then, $\boldsymbol{X}(t)$ is defined as the integral curve of the velocity field,

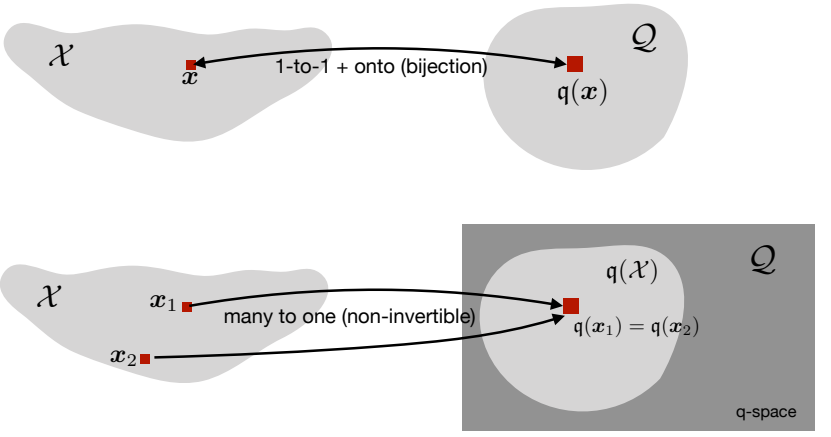

Figure 6: Two cases for the mapping $\mathfrak{q}$ from $\boldsymbol{x}$-space to $\boldsymbol{q}$-space. The top panel shows Case 1. Here, $\mathfrak{q}$ is 1-to-1: each point in the fluid domain, $\boldsymbol{x} \in \mathcal{X}$, is mapped to a unique point $\mathfrak{q}(\boldsymbol{x})$. Also, $\mathfrak{q}$ is onto: for every point $\boldsymbol{q}$ in the codomain of $\mathfrak{q}$, $\mathcal{Q}$, there is at least one point $\boldsymbol{x} \in \mathcal{X}$ that maps to $\boldsymbol{q}$. Together, these properties imply $\mathfrak{q}$ is a *bijection*, with an inverse function mapping from $\mathcal{Q}$ to $\mathcal{X}$. The bottom panel shows Case 2. Here, $\mathfrak{q}$ is not 1-to-1: two elements from $\boldsymbol{x} \in \mathcal{X}$ are mapped to the same point in $\boldsymbol{q}(\mathcal{X})$. Also, $\mathfrak{q}$ is not onto: the function's image, $\mathfrak{q}(\mathcal{X})$, is a strict subset of the function's codomain, $\mathcal{Q}$. Either of these properties prevents $\mathfrak{q}$ from having a well-defined inverse function from $\mathcal{Q}$ to $\mathcal{X}$. Correspondingly, $\mathfrak{q}$ is not a bijection and information is lost by using $\mathfrak{q}$ to map from $\boldsymbol{x}$-space to $\boldsymbol{q}$-space.

$\dot{\boldsymbol{x}}$, through the point $(\boldsymbol{x}_0, t_0)$; that is, $\boldsymbol{X}$ solves the ordinary differential equation

$$\frac{\mathrm{d}\boldsymbol{X}(t)}{\mathrm{d}t} = \dot{\boldsymbol{x}}(\boldsymbol{X}(t), t) \quad \text{with} \quad \boldsymbol{X}(t_0) = \boldsymbol{x}_0. \tag{3.1}$$

Analogously, a trajectory in $\boldsymbol{q}$-space, starting from position $\boldsymbol{q}_0$ at time t_0, is described by a function $\boldsymbol{Q}(t)$ that satisfies $\boldsymbol{Q}(t_0) = \boldsymbol{q}_0$. An example trajectory is depicted in Figure 7. The practical calculation of the trajectory, $\boldsymbol{Q}(t)$, requires knowing the $\boldsymbol{q}$-space velocity, $\dot{\boldsymbol{q}}$, as a field in ($\boldsymbol{q}$-space)-time, i.e. $\dot{\boldsymbol{q}}(\boldsymbol{q}, t)$. Then, $\boldsymbol{Q}$ is defined as the integral curve of the velocity field $\dot{\boldsymbol{q}}$ through the point $(\boldsymbol{q}_0, t_0)$; that is, $\boldsymbol{Q}$ solves the ordinary differential equation

$$\frac{\mathrm{d}\boldsymbol{Q}(t)}{\mathrm{d}t} = \dot{\boldsymbol{q}}(\boldsymbol{Q}(t), t) \quad \text{with} \quad \boldsymbol{Q}(t_0) = \boldsymbol{q}_0. \tag{3.2}$$

Hence, $\dot{\boldsymbol{q}}$ defines the velocity of a trajectory in $\boldsymbol{q}$-space.

Consider Case 1, in which $\mathfrak{q}$ is a bijection that uniquely maps from $\mathcal{X}$ to $\mathcal{Q}$ at each time instance t. This case enables an interpretation of the $\boldsymbol{q}$-space trajectory, $\boldsymbol{Q}(t)$, through the initial point $\boldsymbol{q}_0 = \boldsymbol{Q}(t_0)$: it is simply the $\boldsymbol{q}$ values along the trajectory $\boldsymbol{X}(t)$ through the initial point $(\boldsymbol{x}_0, t_0)$, where $\boldsymbol{x}_0$ is the unique point in $\mathcal{X}$ that has $\mathfrak{q}(\boldsymbol{x}_0) = \boldsymbol{q}_0$ at time t_0. Mathematically,

$$\boldsymbol{Q}(t) = \mathfrak{q}(\boldsymbol{X}(t), t) \quad \text{with} \quad \mathfrak{q}(\boldsymbol{X}(t_0), t_0) = \boldsymbol{q}_0. \tag{3.3}$$

Taking the time derivative of equation (3.3) yields

$$\frac{\mathrm{d}\boldsymbol{Q}(t)}{\mathrm{d}t} = \left[\left.\frac{\partial \mathfrak{q}}{\partial x^a}\right|_{(\boldsymbol{X}(t), t)} \frac{\mathrm{d}X^a(t)}{\mathrm{d}t} + \left.\frac{\partial \mathfrak{q}}{\partial t}\right|_{(\boldsymbol{X}(t), t)} \right] \tag{3.4a}$$

$$= \dot{\mathfrak{q}}(\boldsymbol{X}(t), t) \tag{3.4b}$$

$$= \dot{\boldsymbol{q}}(\boldsymbol{Q}(t), t). \tag{3.4c}$$

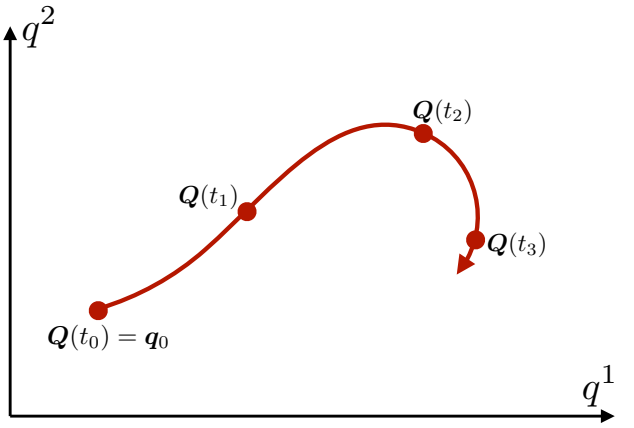

Figure 7: A sample trajectory, $\boldsymbol{Q}(t)$, in an $N = 2$ dimensional fluid property space. We depict positions along the trajectory at four discrete times, with the initial position $\boldsymbol{Q}(t_0) = \boldsymbol{q}_0$.

In equation (3.4*b*), we introduced the function $\dot{\mathbf{q}}(\boldsymbol{x}, t)$ that measures the $\boldsymbol{q}$-space velocity, $\dot{\boldsymbol{q}}$, at each point in the ocean's $\boldsymbol{x}$-space and time domain. In equation (3.4*c*), at a fixed time t, we used the inverse function of $\mathfrak{q}$ to relate $\dot{\boldsymbol{q}}$ at a given $\boldsymbol{q}$ point with $\dot{\mathbf{q}}$ at the unique $\boldsymbol{x}$ point corresponding to $\boldsymbol{q}$; mathematically,

$$\dot{\boldsymbol{q}}(\boldsymbol{q}) = \dot{\mathbf{q}}(\mathfrak{q}^{-1}(\boldsymbol{q})). \tag{3.5}$$

Finally, evaluating equation (3.3) at $t = t_0$ reveals $\boldsymbol{Q}(t_0) = \boldsymbol{q}_0$, and hence equation (3.3) satisfies the definition (3.2).

The interpretation of a $\boldsymbol{q}$-space trajectory as the $\boldsymbol{q}$ values along an $\boldsymbol{x}$-space trajectory (equation (3.3)) does not generalize to Case 2 when $\mathfrak{q}$ is not a 1-to-1 function. The reason this interpretation fails to generalize is that the fluid particles that had $\boldsymbol{q}$ values of $\boldsymbol{q}_0$ at time t_0 will have an assortment of $\boldsymbol{q}$ values at $t \neq t_0$, and hence differ from the set of fluid particles all having the same $\boldsymbol{q}$ value that we collectively use to define $\dot{\boldsymbol{q}}$ (e.g. equations (3.23), (3.28), or (3.34) ahead).

For either Case 1 or Case 2, $\dot{\boldsymbol{q}}$ corresponds to the dia-surface transport discussed in Section 6.7 of Griffies (2004), Figure 3 of Groeskamp *et al.* (2014), and Section 2.1 of Groeskamp *et al.* (2019). In the oceanographic context, we say that $\dot{\boldsymbol{q}}$ measures the transformation of fluid across the respective $\boldsymbol{q}$-space coordinate surface.

3.3. *When $\mathfrak{q}$ is a bijection from $\boldsymbol{x}$-space to $\boldsymbol{q}$-space*

In Case 1, when $N = 3$ and $\mathfrak{q}$ is a bijection (a 1-to-1 and invertible function) from $\mathcal{X}$ to $\mathcal{Q}$, a coordinate transformation connects mathematical expressions written in $\boldsymbol{x}$-space and $\boldsymbol{q}$-space. The inverse mapping $\mathfrak{x}(\boldsymbol{q}) = \mathfrak{q}^{-1}(\boldsymbol{q})$ gives

$$x^a = x^a(q^1, q^2, q^3) \quad \text{for} \quad a = 1, 2, 3 \tag{3.6}$$

where $(x^1, x^2, x^3) = (x, y, z)$ are $\boldsymbol{x}$-space Cartesian coordinates. It then follows that the volume element in $\boldsymbol{x}$-space, $\mathrm{d}V$, is related to that in $\boldsymbol{q}$-space through a coordinate transformation

realized by the chain rule:

$$\mathrm{d}V = \mathrm{d}x^1 \wedge \mathrm{d}x^2 \wedge \mathrm{d}x^3 \tag{3.7a}$$

$$= \frac{\partial x^1}{\partial q^\alpha}\,\mathrm{d}q^\alpha \wedge \frac{\partial x^2}{\partial q^\beta}\,\mathrm{d}q^\beta \wedge \frac{\partial x^3}{\partial q^\gamma}\,\mathrm{d}q^\gamma \tag{3.7b}$$

$$= \mathcal{J}\,\mathrm{d}q^1 \wedge \mathrm{d}q^2 \wedge \mathrm{d}q^3 \tag{3.7c}$$

$$= \mathcal{J}\,\mathrm{d}\mathcal{V}, \tag{3.7d}$$

where repeated indices are summed over their range. Setting $\mathrm{d}V > 0$ fixes the "standard order" convention for the Cartesian coordinate 1-forms, $\mathrm{d}x^a$. We introduced the Jacobian of the transformation, $\mathcal{J}$, which is the determinant of the transformation matrix from $\boldsymbol{q}$-space to Cartesian coordinates used for $\boldsymbol{x}$-space. The Jacobian is written in the form

$$\mathcal{J} = \det\left(\frac{\partial x^a}{\partial q^\alpha}\right) = \frac{\partial \boldsymbol{x}}{\partial \boldsymbol{q}}, \tag{3.8}$$

where we introduce the shorthand for the scalar triple product (e.g., Section 1.2 of Salmon (1998))

$$\frac{\partial \boldsymbol{x}}{\partial \boldsymbol{q}} = \left[\frac{\partial \boldsymbol{x}}{\partial q^1} \times \frac{\partial \boldsymbol{x}}{\partial q^2}\right] \cdot \frac{\partial \boldsymbol{x}}{\partial q^3} = \left[\frac{\partial x^1}{\partial \boldsymbol{q}} \times \frac{\partial x^2}{\partial \boldsymbol{q}}\right] \cdot \frac{\partial x^3}{\partial \boldsymbol{q}}, \tag{3.9}$$

with $\times$ the vector cross product. By the inverse function theorem, $\mathcal{J} \neq 0$ for all $x \in \mathcal{X}$ — under the present assumption that $\mathfrak{q}$ is bijective from $\mathcal{X}$ to $\mathcal{Q}$. Having assumed that $\mathfrak{q}$ is continuously differentiable, then $\mathcal{J}$ is continuous, so $\mathcal{J} \neq 0$ further implies that $\mathcal{J}$ is single-signed. If $\mathcal{J} > 0$ then the coordinate transformation is orientation preserving, whereas $\mathcal{J} < 0$ swaps the orientation.

The Jacobian is central to how we connect physical objects represented in $\boldsymbol{x}$-space to their representation in $\boldsymbol{q}$-space. Geometrically, the Jacobian measures the ratio of the volume elements for the respective coordinates

$$\mathcal{J} = \mathrm{d}V/\mathrm{d}\mathcal{V}, \tag{3.10}$$

and in so doing it converts between physical dimensions. To illustrate this conversion, consider the mass of an elemental fluid region written in the equivalent manners

$$\mathrm{d}M = \mathfrak{m}\,|\mathrm{d}\mathcal{V}| = \rho\,\mathrm{d}V, \tag{3.11}$$

with $\rho(\boldsymbol{x}, t)$ the mass per unit volume in $\boldsymbol{x}$-space. The absolute value in equation (3.11) is needed because $\mathrm{d}M$ and $\mathfrak{m}$ are positive semi-definite but $\mathrm{d}\mathcal{V}$ is not necessarily so. We are thus led to the corresponding relation between the mass per unit volume in $\boldsymbol{x}$-space, $\rho(\boldsymbol{x}, t)$ and the mass density in $\boldsymbol{q}$-space, $\mathfrak{m}$:

$$\mathfrak{m} = \rho\,|\mathcal{J}|, \tag{3.12}$$

evaluated at an arbitrary $\boldsymbol{q}$. In particular, ρ evaluated at $\boldsymbol{q}$ is just ρ evaluated at the unique point $\boldsymbol{x}$ satisfying $\mathfrak{q}(\boldsymbol{x}) = \boldsymbol{q}$, i.e. $\rho(\boldsymbol{q}) = \rho(\mathfrak{q}^{-1}(\boldsymbol{q}))$, akin to (3.5). Recall that for an oceanic Boussinesq fluid, mass conservation becomes volume conservation whereby ρ is replaced by a global constant, ρ_0. Even so, the mass density in $\boldsymbol{q}$-space is generally not a constant due to the non-constant Jacobian.

When $\mathfrak{q}$ is a bijection, then $\boldsymbol{q}$-space inherits a full metric structure from $\boldsymbol{x}$-space, and retains the positive definite determinant of the metric tensor. Hence, infinitesimal distances in $\boldsymbol{x}$-space are given in terms of displacements in $\boldsymbol{q}$-space, by

$$(\mathrm{d}s)^2 = (\mathrm{d}\boldsymbol{x} \cdot \mathrm{d}\boldsymbol{x}) = \mathrm{d}q^\alpha\, g_{\alpha\beta}\, \mathrm{d}q^\beta \tag{3.13}$$

where

$$g_{\alpha\beta} = \frac{\partial \boldsymbol{x}}{\partial q^\alpha} \cdot \frac{\partial \boldsymbol{x}}{\partial q^\beta} = \frac{\partial x^a}{\partial q^\alpha} \frac{\partial x^a}{\partial q^\beta} \tag{3.14}$$

is the covariant expression of the metric tensor. It follows that the Jacobian is related to the determinant of $g_{\alpha\beta}$ via

$$|\mathcal{J}| = \sqrt{\det(g_{\alpha\beta})}. \tag{3.15}$$

3.4. *When the mapping from $\boldsymbol{x}$-space to $\boldsymbol{q}$-space is not 1-to-1*

We now consider the more general case when $\mathfrak{q}$ is not a 1-to-1 function from $\mathcal{X}$ to $\mathcal{Q}$. In this case, no global $\mathfrak{x}(\boldsymbol{q}) = \mathfrak{q}^{-1}(\boldsymbol{q})$ exists, and so there is no distance metric or metric tensor. However, it is still possible to define a generalized Jacobian that links the volume elements in $\boldsymbol{q}$-space and $\boldsymbol{x}$-space.

We develop the theory first by patching together results from the previous subsection for regions within which $\mathfrak{q}$ is 1-to-1, and then by summing or integrating over the entire discrete or continuous domain while employing a boxcar or Dirac delta to select only those points in $\boldsymbol{x}$-space with a given $\boldsymbol{q}$ value.

3.4.1. *Patching regions that are not 1-to-1*

To use the theory of Section 3.3, we continue with the special case of $N = 3$ for now. The fluid domain $\mathcal{X}$, assumed finite, can be partitioned into a finite set of regions within each of which $\mathfrak{q}$ is 1-to-1. Now, considering a point $\tilde{\boldsymbol{q}} \in \mathcal{Q}$, there is at most one point $\boldsymbol{x}$ that maps to $\tilde{\boldsymbol{q}}$ in each region. Thus, there are a finite number of points in $\boldsymbol{x}$-space, enumerated $\boldsymbol{x}_I$ for $I = 1, \ldots, N_\mathrm{P}$, where $\mathfrak{q}(\boldsymbol{x}_I) = \tilde{\boldsymbol{q}}$. Note that N_P depends on $\tilde{\boldsymbol{q}}$. Moreover, assume $\mathcal{G}(\boldsymbol{x}_I) \neq 0$ for each $\boldsymbol{x}_I$, where

$$\mathcal{G}(\tilde{\boldsymbol{x}}) = \left.\frac{\partial \mathfrak{q}}{\partial \boldsymbol{x}}\right|_{\boldsymbol{x}=\tilde{\boldsymbol{x}}} \tag{3.16}$$

is the inverse Jacobian, i.e. the Jacobian for the mapping $\mathfrak{q}$ from $\boldsymbol{x}$-space to $\boldsymbol{q}$-space. By the inverse function theorem, there exists a small neighborhood, $B(\boldsymbol{x}_I) \subset \mathcal{X}$, with $\boldsymbol{x}_I \in B(\boldsymbol{x}_I)$ and for which the restriction of $\mathfrak{q}$ to $B(\boldsymbol{x}_I)$, denoted $\mathfrak{q}_I : B(\boldsymbol{x}_I) \to \mathfrak{q}(B(\boldsymbol{x}_I))$, is invertible. The inverse of $\mathfrak{q}_I$ satisfies $\mathfrak{q}_I^{-1}(\tilde{\boldsymbol{q}}) = \boldsymbol{x}_I$ and so can be used to evaluate the density at $\tilde{\boldsymbol{q}}$ for the I'th region,

$$\rho_I(\tilde{\boldsymbol{q}}) = \rho(\mathfrak{q}_I^{-1}(\tilde{\boldsymbol{q}})), \tag{3.17}$$

and likewise the $\boldsymbol{q}$-space velocity at $\tilde{\boldsymbol{q}}$ for the I'th region,

$$\dot{\boldsymbol{q}}_I(\tilde{\boldsymbol{q}}) = \dot{\mathfrak{q}}\big(\mathfrak{q}_I^{-1}(\tilde{\boldsymbol{q}})\big). \tag{3.18}$$

Similarly, $\mathfrak{q}_I^{-1}$ defines the Jacobian of the mapping from $\boldsymbol{q}$-space to $\boldsymbol{x}$-space at each $\boldsymbol{x}_I$:

$$\mathcal{J}_I(\tilde{\boldsymbol{q}}) = \left.\frac{\partial \mathfrak{x}_I}{\partial \boldsymbol{q}}\right|_{\boldsymbol{q}=\tilde{\boldsymbol{q}}} \qquad \text{where} \qquad \mathfrak{x}_I(\boldsymbol{q}) = \mathfrak{q}_I^{-1}(\boldsymbol{q}). \tag{3.19}$$

By the inverse function theorem, $\mathcal{J}_I(\tilde{\boldsymbol{q}}) = 1/\mathcal{G}(\boldsymbol{x}_I)$. Note that the N_P values of $\mathcal{J}_I(\tilde{\boldsymbol{q}})$ need not all have the same sign.

Patching together information about the separate N_P regions, we define the generalized Jacobian at $\tilde{\boldsymbol{q}}$ as the discrete sum of the volume ratios for each region,

$$\mathcal{J}^{\mathrm{gen}}(\tilde{\boldsymbol{q}}) = \sum_{I=1}^{N_\mathrm{P}} |\mathcal{J}_I(\tilde{\boldsymbol{q}})|. \tag{3.20}$$

Similarly, the generalized $\boldsymbol{x}$-space mass density at $\tilde{\boldsymbol{q}}$ is

$$\rho^{\text{gen}}(\tilde{\boldsymbol{q}}) = \frac{1}{\mathcal{J}^{\text{gen}}(\tilde{\boldsymbol{q}})} \sum_{I=1}^{N_{\text{P}}} \rho_I(\tilde{\boldsymbol{q}})\, |\mathcal{J}_I(\tilde{\boldsymbol{q}})|, \tag{3.21}$$

so that the generalized $\boldsymbol{q}$-space mass density at $\tilde{\boldsymbol{q}}$ is

$$\mathfrak{m}^{\text{gen}}(\tilde{\boldsymbol{q}}) = \rho^{\text{gen}}(\tilde{\boldsymbol{q}})\, \mathcal{J}^{\text{gen}}(\tilde{\boldsymbol{q}}) \tag{3.22a}$$

$$= \sum_{I=1}^{N_{\text{P}}} \rho_I(\tilde{\boldsymbol{q}})\, \big|\mathcal{J}_I(\tilde{\boldsymbol{q}})\big|. \tag{3.22b}$$

Equation (3.22*a*) generalizes equation (3.12) that holds when $\mathfrak{q}$ is bijective. Equation (3.22*b*) represents the generalized $\boldsymbol{q}$-space mass density as a discrete sum of the individual $\boldsymbol{q}$-space mass densities for each region. The mass density, $\mathfrak{m}^{\text{gen}}$, is analogous to the mass density for a multi-component fluid with N_{P} components each with mass density $\rho_I|\mathcal{J}_I|$ (e.g., Section 11.11 of Aris 1962), only here with the components represented by fluid from different $\boldsymbol{x}$-space patches. In a similar manner, the generalized $\boldsymbol{q}$-space velocity is constructed as a mass-weighted average of the $\boldsymbol{q}$-space velocities from individual regions (each given by equation (3.5)),

$$\dot{\boldsymbol{q}}^{\text{gen}}(\tilde{\boldsymbol{q}}) = \frac{1}{\mathfrak{m}^{\text{gen}}(\tilde{\boldsymbol{q}})} \sum_{I=1}^{N_{\text{P}}} \dot{\boldsymbol{q}}_I(\tilde{\boldsymbol{q}})\, \rho_I(\tilde{\boldsymbol{q}})\, \big|\mathcal{J}_I(\tilde{\boldsymbol{q}})\big|. \tag{3.23}$$

At special points where the inverse Jacobian, $\mathcal{G}$, is zero, $\mathcal{J}_I(\tilde{\boldsymbol{q}})$ is infinite and hence so too are $\mathcal{J}^{\text{gen}}(\tilde{\boldsymbol{q}})$ and $\mathfrak{m}^{\text{gen}}(\tilde{\boldsymbol{q}})$. We say more about this situation in Section 3.4.2, where we show that this situation does not indicate a failure of the theory.

Next, we generalize these results to the case in which the dimension N of $\boldsymbol{q}$-space is arbitrary, first with a binning procedure appropriate for discrete data and then for the continuous limit.

3.4.2. *Generalized transformations with discrete data*

Consider a discretized fluid domain, $\mathcal{X}$, that is composed of elementary regions of $\boldsymbol{x}$-space (still denoted $\boldsymbol{x} \in \mathcal{X}$), each with a specified positive volume, $\Delta V(\boldsymbol{x})$. Similarly, consider discretizing $\boldsymbol{q}$-space into bins. Let the bin centered at $\tilde{\boldsymbol{q}}$ be the set $\mathcal{B}(\tilde{\boldsymbol{q}}) \subset \mathcal{Q}$ and have a finite and positive $\boldsymbol{q}$-space volume of $\Delta\mathcal{V}(\tilde{\boldsymbol{q}})$. There may be an arbitrary number of elementary $\boldsymbol{x}$-space regions that map to $\mathcal{B}(\tilde{\boldsymbol{q}})$. At any time instance, we define the generalized Jacobian as the volume ratio of these regions,

$$\mathcal{J}^{\text{gen}}(\tilde{\boldsymbol{q}}) = \frac{1}{\Delta\mathcal{V}(\tilde{\boldsymbol{q}})} \sum_{\boldsymbol{x}\in\mathcal{X}} \Delta V(\boldsymbol{x})\, \Pi_{\tilde{\boldsymbol{q}}}\big(\mathfrak{q}(\boldsymbol{x})\big), \tag{3.24}$$

where the sum extends over all points within the discretized ocean, $\boldsymbol{x} \in \mathcal{X}$, and where we introduced the dimensionless boxcar function (e.g., equation (46) of Groeskamp *et al.* (2019))

$$\Pi_{\tilde{\boldsymbol{q}}}(\boldsymbol{q}) = \begin{cases} 1 & \text{if } \boldsymbol{q} \in \mathcal{B}(\tilde{\boldsymbol{q}}) \\ 0 & \text{otherwise.} \end{cases} \tag{3.25}$$

Note that $\mathcal{J}^{\text{gen}}(\tilde{\boldsymbol{q}}) = 0$ if $\mathfrak{q}(\boldsymbol{x}) \notin \mathcal{B}(\tilde{\boldsymbol{q}})$ for all $\boldsymbol{x} \in \mathcal{X}$, i.e. if the bin centered at $\tilde{\boldsymbol{q}}$ is not mapped to by any point in $\boldsymbol{x}$-space.

The generalized $\boldsymbol{x}$-space mass density at $\tilde{\boldsymbol{q}}$ is defined as the mass in all elementary regions

$\boldsymbol{x}$ for which $\mathfrak{q}(\boldsymbol{x}) \in \mathcal{B}(\tilde{\boldsymbol{q}})$ divided by the total $\boldsymbol{x}$-space volume of the same regions,

$$\rho^{\text{gen}}(\tilde{\boldsymbol{q}}) = \frac{\sum_{\boldsymbol{x}\in\mathcal{X}} \rho(\boldsymbol{x})\,\Delta V(\boldsymbol{x})\,\Pi_{\tilde{\boldsymbol{q}}}\big(\mathfrak{q}(\boldsymbol{x})\big)}{\Delta\mathcal{V}(\tilde{\boldsymbol{q}})\;\mathcal{J}^{\text{gen}}(\tilde{\boldsymbol{q}})}. \tag{3.26}$$

The definition (3.26) holds if there is at least one point, $\boldsymbol{x} \in \mathcal{X}$, such that $\mathfrak{q}(\boldsymbol{x}) \in \mathcal{B}(\tilde{\boldsymbol{q}})$, whereas $\rho^{\text{gen}}(\tilde{\boldsymbol{q}}) = 0$ otherwise. Analogously, the generalized $\boldsymbol{q}$-space mass density at $\tilde{\boldsymbol{q}}$ is the total mass in elementary regions $\boldsymbol{x}$ where $\mathfrak{q}(\boldsymbol{x}) = \tilde{\boldsymbol{q}}$ divided by the $\boldsymbol{q}$-space volume of the bin centered at $\tilde{\boldsymbol{q}}$,

$$\mathfrak{m}^{\text{gen}}(\tilde{\boldsymbol{q}}) = \frac{1}{\Delta\mathcal{V}(\tilde{\boldsymbol{q}})} \sum_{\boldsymbol{x}\in\mathcal{X}} \rho(\boldsymbol{x})\,\Delta V(\boldsymbol{x})\,\Pi_{\tilde{\boldsymbol{q}}}\big(\mathfrak{q}(\boldsymbol{x})\big) \tag{3.27a}$$

$$= \rho^{\text{gen}}(\tilde{\boldsymbol{q}})\;\mathcal{J}^{\text{gen}}(\tilde{\boldsymbol{q}}). \tag{3.27b}$$

Like $\mathcal{J}^{\text{gen}}$, note that $\mathfrak{m}^{\text{gen}}(\tilde{\boldsymbol{q}}) = 0$ if $\mathfrak{q}(\boldsymbol{x}) \notin \mathcal{B}(\tilde{\boldsymbol{q}})$ for all $\boldsymbol{x} \in \mathcal{X}$. Finally, the generalized $\boldsymbol{q}$-space velocity at $\tilde{\boldsymbol{q}}$ is the mass-weighted average of $\dot{\boldsymbol{q}}$ over regions $\boldsymbol{x} \in \mathcal{X}$ where $\mathfrak{q}(\boldsymbol{x}) \in \mathcal{B}(\tilde{\boldsymbol{q}})$,

$$\dot{\boldsymbol{q}}^{\text{gen}}(\tilde{\boldsymbol{q}}) = \frac{\sum_{\boldsymbol{x}\in\mathcal{X}} \dot{\mathfrak{q}}(\boldsymbol{x})\,\rho(\boldsymbol{x})\,\Delta V(\boldsymbol{x})\,\Pi_{\tilde{\boldsymbol{q}}}\big(\mathfrak{q}(\boldsymbol{x})\big)}{\Delta\mathcal{V}(\tilde{\boldsymbol{q}})\;\mathfrak{m}^{\text{gen}}(\tilde{\boldsymbol{q}})}. \tag{3.28}$$

The definition (3.28) holds if there is at least one point $\boldsymbol{x} \in \mathcal{X}$ with $\mathfrak{q}(\boldsymbol{x}) \in \mathcal{B}(\tilde{\boldsymbol{q}})$, whereas $\dot{\boldsymbol{q}}^{\text{gen}}(\tilde{\boldsymbol{q}}) = 0$ otherwise.

To illuminate the issue raised in Section 3.4.1 — that the Jacobian $\mathcal{J}$ can be infinite at points where the inverse Jacobian $\mathcal{G}$ is zero — consider an example where $\boldsymbol{q} = \Theta$ and imagine $\Theta = 20°\text{C}$ in the entire fluid domain. The discretized, generalized Jacobian, $\mathcal{J}^{\text{gen}}$, is zero for each bin except for the one and only bin containing 20°C, where the value of $\mathcal{J}^{\text{gen}}$ is the volume of the entire fluid (in m^3) divided by the volume of this $\boldsymbol{q}$-space bin ($\Delta\mathcal{V} = \Delta\Theta$). As the size of this bin is reduced ($\Delta\Theta \to 0°\text{C}$), the value of $\mathcal{J}^{\text{gen}}$ for the single bin containing 20°C increases towards infinity, but in such a way that $\mathcal{J}^{\text{gen}}\,\Delta\Theta$ remains finite — namely, the volume of the entire fluid. A similar discussion applies to $\mathfrak{m}^{\text{gen}}$, replacing "volume of the entire fluid" by "mass of the entire fluid". On the other hand, the value of ρ^{gen} in the bin containing 20°C remains finite as the $\boldsymbol{q}$-space bin volume is reduced toward zero: it is the average mass density of the entire fluid. Likewise, $\dot{\boldsymbol{q}}^{\text{gen}}$ also remains finite for the bin containing 20°C: it is the mass-weighted average $\dot{\boldsymbol{q}}$ of the entire fluid. While this discussion illuminates the behavior of these functions as $\Delta\mathcal{V}(\tilde{\boldsymbol{q}}) \to 0$, any individual discretization will have $\Delta\mathcal{V}(\tilde{\boldsymbol{q}}) > 0$, and so the above functions, for the case of discrete data, are finite-valued.

3.4.3. *Generalized transformations in the continuum*

Continuing the case of arbitrary N-dimensional $\boldsymbol{q}$-space, we now consider the continuum limit, wherein the bin sizes are infinitesimal. In this limit, we integrate over $\mathcal{X}$ rather than sum over elementary regions, and the boxcar function is traded for a Dirac delta according to the identity (e.g. Appendix II of Cohen-Tannoudji *et al.* 1977)

$$\delta_{\tilde{\boldsymbol{q}}}(\boldsymbol{q}) = \lim_{\Delta\mathcal{V}(\tilde{\boldsymbol{q}})\to 0} \frac{\Pi_{\tilde{\boldsymbol{q}}}(\boldsymbol{q})}{\Delta\mathcal{V}(\tilde{\boldsymbol{q}})}. \tag{3.29}$$

The Dirac delta, $\delta_{\tilde{\boldsymbol{q}}}$, carries dimensions of $\mathcal{V}^{-1}$ and is marked to a specific point $\tilde{\boldsymbol{q}}$ (rather than to the origin, as the manifold $\mathcal{Q}$ lacks the notion of an origin). Multiplying equation (3.29) by a smooth function, $f(\boldsymbol{q})$, and integrating over $\mathcal{Q}$ reveals that $\delta_{\tilde{\boldsymbol{q}}}$ satisfies the sifting

property,

$$\int_{\mathcal{Q}} f(\boldsymbol{q})\, \delta_{\tilde{\boldsymbol{q}}}(\boldsymbol{q})\, \mathrm{d}\mathcal{V} = \begin{cases} f(\tilde{\boldsymbol{q}}) & \text{if } \tilde{\boldsymbol{q}} \in \mathcal{Q} \\ 0 & \text{if } \tilde{\boldsymbol{q}} \notin \mathcal{Q}. \end{cases} \tag{3.30}$$

Choosing $f(\boldsymbol{q}) = 1$ reveals how $\delta_{\tilde{\boldsymbol{q}}}$ is normalized, integrating to 1 if $\tilde{\boldsymbol{q}} \in \mathcal{Q}$, otherwise integrating to 0.

In the continuum limit, the generalized Jacobian from equation (3.24) becomes

$$\mathcal{J}^{\text{gen}}(\tilde{\boldsymbol{q}}) = \int_{\mathcal{X}} \delta_{\tilde{\boldsymbol{q}}}\big(\mathfrak{q}(\boldsymbol{x})\big)\, \mathrm{d}V. \tag{3.31}$$

Note that $\mathcal{J}^{\text{gen}}(\tilde{\boldsymbol{q}}) = 0$ if $\tilde{\boldsymbol{q}} \notin \mathfrak{q}(\mathcal{X})$ — that is, if $\tilde{\boldsymbol{q}}$ is not mapped to by any point $\boldsymbol{x} \in \mathcal{X}$. Similarly, for all points $\tilde{\boldsymbol{q}} \in \mathfrak{q}(\mathcal{X})$, the generalized $\boldsymbol{x}$-space mass density at $\tilde{\boldsymbol{q}}$ from equation (3.26), the generalized $\boldsymbol{q}$-space mass density from equation (3.27), and the generalized $\boldsymbol{q}$-space velocity from equation (3.28), each become

$$\rho^{\text{gen}}(\tilde{\boldsymbol{q}}) = \frac{1}{\mathcal{J}^{\text{gen}}(\tilde{\boldsymbol{q}})} \int_{\mathcal{X}} \rho(\boldsymbol{x})\, \delta_{\tilde{\boldsymbol{q}}}\big(\mathfrak{q}(\boldsymbol{x})\big)\, \mathrm{d}V, \tag{3.32}$$

$$\mathfrak{m}^{\text{gen}}(\tilde{\boldsymbol{q}}) = \int_{\mathcal{X}} \rho(\boldsymbol{x})\, \delta_{\tilde{\boldsymbol{q}}}\big(\mathfrak{q}(\boldsymbol{x})\big)\, \mathrm{d}V \tag{3.33a}$$

$$= \rho^{\text{gen}}(\tilde{\boldsymbol{q}})\, \mathcal{J}^{\text{gen}}(\tilde{\boldsymbol{q}}), \tag{3.33b}$$

$$\dot{\boldsymbol{q}}^{\text{gen}}(\tilde{\boldsymbol{q}}) = \frac{1}{\mathfrak{m}^{\text{gen}}(\tilde{\boldsymbol{q}})} \int_{\mathcal{X}} \dot{\mathfrak{q}}(\boldsymbol{x})\, \rho(\boldsymbol{x})\, \delta_{\tilde{\boldsymbol{q}}}\big(\mathfrak{q}(\boldsymbol{x})\big)\, \mathrm{d}V. \tag{3.34}$$

If $\tilde{\boldsymbol{q}} \notin \mathfrak{q}(\mathcal{X})$, then $\rho^{\text{gen}}(\tilde{\boldsymbol{q}}) = 0$, $\mathfrak{m}^{\text{gen}}(\tilde{\boldsymbol{q}}) = 0$, and $\dot{\boldsymbol{q}}^{\text{gen}}(\tilde{\boldsymbol{q}}) = 0$.

If $\tilde{\boldsymbol{q}} = \mathfrak{q}(\boldsymbol{x})$ for some $\boldsymbol{x}$ at which $\mathcal{G}(\boldsymbol{x}) = 0$, then $\mathcal{J}^{\text{gen}}(\tilde{\boldsymbol{q}})$ is, loosely speaking, infinite. (This singular behavior arises via the composition of the Dirac delta with $\mathfrak{q}(\boldsymbol{x})$ in equation (3.31), which can be re-expressed as the Dirac delta divided by $|\mathcal{G}|$.) However, this singularity is controlled, in that the integral of $\mathcal{J}^{\text{gen}}$ over a region of $\boldsymbol{q}$-space remains finite. This situation is analogous to how the integral of the Dirac delta $\delta_{\tilde{\boldsymbol{q}}}$ is finite, despite $\delta_{\tilde{\boldsymbol{q}}}$ being "infinite" at $\tilde{\boldsymbol{q}}$. Mathematically, $\mathcal{J}^{\text{gen}}$ is, like $\delta_{\tilde{\boldsymbol{q}}}$, a *distribution* or a *generalized function* rather than a function in the ordinary sense (e.g., see Chapter 1 in Stakgold (2000*a*) and Chapter 5 in Stakgold (2000*b*)). Returning to the example of $\boldsymbol{q} = \Theta$ and a fluid of uniform $\Theta = 20°\text{C}$ but now in the continuum case, what matters is that $\int_a^b \mathcal{J}^{\text{gen}}(\Theta)\, \mathrm{d}\Theta$ returns the volume of the entire fluid domain if $20°\text{C} \in [a, b]$ and returns 0 otherwise.

3.4.4. *Notation convention*

In the following, we make use of the more succinct notation from Section 3.3, effectively dropping the "gen" superscripts. Yet when $\mathfrak{q}$ is not a bijection, we assume the formalism of the present subsection (either the discrete or continuum case as appropriate) has been used to compute the generalized Jacobian, generalized mass density, and generalized $\boldsymbol{q}$-space velocity. In so doing, the formulation in the following sections is appropriate whether $\mathfrak{q}$ is bijective or not.

3.5. *Boundaries in $\boldsymbol{q}$-space*

Boundaries in $\boldsymbol{x}$-space are specified by the geometry of the domain, $\mathcal{X}$, containing the fluid. For example, the sea floor and sea surface make up the oceanic boundary. If, at each time t, the function $\mathfrak{q}$ is bijective from $\mathcal{X}$ to $\mathcal{Q}$ (Case 1), then boundaries of $\mathcal{X}$ correspond to boundaries of $\mathcal{Q}$. However, in the absence of a 1-to-1 mapping from $\mathcal{X}$ to $\mathcal{Q}$ (Case 2), $\boldsymbol{q}$-space has no

direct information about the geometry of the $\boldsymbol{x}$-space fluid domain. Hence, boundaries in $\boldsymbol{q}$-space need to be treated differently from those in $\boldsymbol{x}$-space. With our choice for Case 2 that $\mathcal{Q}$ is all of $\boldsymbol{q}$-space (Section 3.1), the boundaries of $\mathcal{X}$ correspond to points in the interior of $\mathcal{Q}$. As such, $\boldsymbol{x}$-space boundary fluxes must appear as source terms in $\boldsymbol{q}$-space. For example, a mass flux (e.g., evaporation, precipitation) that crosses the boundary of the ocean domain, $\partial\mathcal{X}$, appears as a source in $\boldsymbol{q}$-space at the $\boldsymbol{q}$-space value of the point in $\boldsymbol{x}$-space where the mass enters. Likewise, for tracers used to define $\boldsymbol{q}$-space coordinates, the $\boldsymbol{x}$-space boundary tracer flux appears as a corresponding $\boldsymbol{q}$-space source.

4. Mass conservation

There have been two approaches to working with fluid property space. In the treatments of Marshall *et al.* (1999), Iudicone *et al.* (2008) and Groeskamp *et al.* (2019), the integration and differentiation are performed in $\boldsymbol{x}$-space and the results transformed to $\boldsymbol{q}$-space. In contrast, in the treatment of Walin (1977) and, for example, Nurser *et al.* (1999), volume elements, diabatic forcing, fluxes, and other quantities are first projected onto $\boldsymbol{q}$-space and the budgets also performed in $\boldsymbol{q}$-space. We here follow the $\boldsymbol{q}$-space approach, offering further rigour to the method and extending it to $\boldsymbol{q}$-space with arbitrary dimension, N.

4.1. *Mass transport exterior form*

We here make use of exterior forms (Appendix B) since they do not rely on a metric structure. To derive the mass budget for a region fixed in $\boldsymbol{q}$-space, we introduce the mass transport exterior form that measures the oriented mass transport through an N-1 dimensional surface. The formalism holds for an arbitrary number of $\boldsymbol{q}$-space dimensions, and we display results for $N = 1, 2, 3$.

Starting with $N = 3$ we introduce the mass transport 2-form

$$\mathcal{T} = \mathfrak{m}\,(\dot{q}^1\, \mathrm{d}q^2 \wedge \mathrm{d}q^3 + \dot{q}^2\, \mathrm{d}q^3 \wedge \mathrm{d}q^1 + \dot{q}^3\, \mathrm{d}q^1 \wedge \mathrm{d}q^2), \tag{4.1}$$

with $\mathcal{T}$ having dimensions of mass per time. Following Section 2.9b of Frankel (2012), we mathematically interpret $\mathcal{T}$ as the interior product (see also Appendix B.3) of the vector $\mathfrak{m}\,\dot{\boldsymbol{q}}$ with the volume N-form $\mathrm{d}\mathcal{V}$. Thus equation (4.1) follows from equations (B 9) and (B 10). Physically, we interpret $\mathfrak{m}\,\dot{q}^1\, \mathrm{d}q^2 \wedge \mathrm{d}q^3$ as the mass transport (mass per time) penetrating the infinitesimal surface element in $\boldsymbol{q}$-space defined by $\mathrm{d}q^2 \wedge \mathrm{d}q^3$. We take the right hand convention so that a positive $\dot{q}^1$ leads to mass transport from the negative side to the positive side of the infinitesimal surface defined by $\mathrm{d}q^2$ and $\mathrm{d}q^3$. Analogous interpretations hold for the other two terms. Also, recall the geometric interpretation in Figure 5 for the area element 2-form for the special case of Cartesian coordinates; this interpretation extends to the arbitrary coordinates of $\boldsymbol{q}$-space.

For $N = 2$, the interior product equation (B 9) gives the mass transport 1-form as

$$\mathcal{T} = \mathfrak{m}\,\epsilon_{\alpha\beta}\dot{q}^\alpha\, \mathrm{d}q^\beta = \mathfrak{m}\,(\dot{q}^1\, \mathrm{d}q^2 - \dot{q}^2\, \mathrm{d}q^1), \tag{4.2}$$

where we used the properties of the permutation symbol, $\epsilon_{12} = -\epsilon_{21} = 1$ and $\epsilon_{11} = \epsilon_{22} = 0$. For example, with $(q^1, q^2) = (S, \Theta)$, the mass transport 1-form is given by

$$\mathcal{T} = \mathfrak{m}\,(\dot{S}\, \mathrm{d}\Theta - \dot{\Theta}\, \mathrm{d}S). \tag{4.3}$$

With $N = 1$ we make use of the mass transport 0-form given by

$$\mathcal{T} = \mathfrak{m}\,\dot{q}. \tag{4.4}$$

In this case, flow occurs along the single coordinate direction. For example, when binning the fluid according to temperature, then $\mathcal{T} = \mathfrak{m}\,\dot{\Theta}$.

4.2. *Deriving the mass continuity equation*

We here develop the mass continuity equation, which is the continuum budget for mass contained in an infinitesimal elemental region fixed in $\boldsymbol{q}$-space. That is, we want to determine what affects the time derivative

$$\partial_t(\mathrm{d}M) = \partial_t(\mathfrak{m}\,\mathrm{d}\mathcal{V}) = (\partial_t \mathfrak{m})\,\mathrm{d}\mathcal{V}, \tag{4.5}$$

where the time derivative is computed holding the $\boldsymbol{q}$-coordinates fixed so that $\partial_t(\mathrm{d}\mathcal{V}) = 0$.

Just as when developing the Eulerian mass budget for $\boldsymbol{x}$-space, we presume that the mass of an elemental region of $\boldsymbol{q}$-space is affected by the accumulation of mass transported into the volume of $\boldsymbol{q}$-space, along with any mass sources. These considerations lead us to formulate the mass budget for an elemental volume in $\boldsymbol{q}$-space in the generic manner

$$(\partial_t \mathfrak{m})\,\mathrm{d}\mathcal{V} = -\mathrm{d}\mathcal{T} + \mathcal{M}\,\mathrm{d}\mathcal{V} \tag{4.6}$$

with the $\boldsymbol{q}$-space mass source (mass per time) given by $\mathcal{M}\,\mathrm{d}\mathcal{V}$, and with $\mathrm{d}\mathcal{T}$ the spatial exterior derivative of the mass transport exterior form.

We derive a more conventional form of the mass continuity equation (4.6) by considering the case of $N = 2$, in which the spatial exterior derivative of the transport 1-form is given by (see Appendix B.4 for details)

$$\begin{aligned}
\mathrm{d}\mathcal{T} &= \mathrm{d}\left[\mathfrak{m}\,\dot{q}^1\,\mathrm{d}q^2 - \mathfrak{m}\,\dot{q}^2\,\mathrm{d}q^1\right] && (4.7a)\\
&= \partial_{q^1}(\mathfrak{m}\,\dot{q}^1)\,\mathrm{d}q^1 \wedge \mathrm{d}q^2 - \partial_{q^2}(\mathfrak{m}\,\dot{q}^2)\,\mathrm{d}q^2 \wedge \mathrm{d}q^1 && (4.7b)\\
&= [\partial_{q^1}(\mathfrak{m}\,\dot{q}^1) + \partial_{q^2}(\mathfrak{m}\,\dot{q}^2)]\,\mathrm{d}q^1 \wedge \mathrm{d}q^2 && (4.7c)\\
&= [\partial_{q^1}(\mathfrak{m}\,\dot{q}^1) + \partial_{q^2}(\mathfrak{m}\,\dot{q}^2)]\,\mathrm{d}\mathcal{V}. && (4.7d)
\end{aligned}$$

In the above we noted that anti-symmetry of the exterior product means that

$$\mathrm{d}q^1 \wedge \mathrm{d}q^1 = \mathrm{d}q^2 \wedge \mathrm{d}q^2 = 0. \tag{4.8}$$

Furthermore, we used the property of the exterior derivative, whereby it is an anti-symmetrized derivative operator so that the exterior derivative of a p-form produces a $(p+1)$-form. Using $\mathrm{d}\mathcal{T}$ in the form of equation (4.7d) in the mass continuity equation (4.6), and then cancelling the common $\mathrm{d}\mathcal{V}$ factor, leads to the $\boldsymbol{q}$-space mass continuity equation

$$\partial_t \mathfrak{m} = -\partial_{q^1}(\mathfrak{m}\,\dot{q}^1) - \partial_{q^2}(\mathfrak{m}\,\dot{q}^2) + \mathcal{M}. \tag{4.9}$$

This result readily generalizes to arbitrary dimensions of $\boldsymbol{q}$-space

$$\partial_t \mathfrak{m} = -\partial_\alpha(\mathfrak{m}\,\dot{q}^\alpha) + \mathcal{M} = -\boldsymbol{\nabla}_{\boldsymbol{q}} \cdot (\mathfrak{m}\,\dot{\boldsymbol{q}}) + \mathcal{M}. \tag{4.10}$$

The second equality introduced the operator, $\boldsymbol{\nabla}_{\boldsymbol{q}}$, as a shorthand for the partial derivative operators along $\boldsymbol{q}$-space coordinates. The flux-form continuity equation (4.10) can be written in the equivalent advective form by expanding the $\partial/\partial q^\alpha$ derivatives

$$(\partial_t + \dot{q}^\alpha\,\partial_\alpha)\,\mathfrak{m} = -\mathfrak{m}\,\partial_\alpha \dot{q}^\alpha + \mathcal{M}. \tag{4.11}$$

The mass continuity equation (4.10) reveals that the $\boldsymbol{q}$-space mass density, $\mathfrak{m}$, changes in time within a fixed $\boldsymbol{q}$-space elemental region according to mass sources as well as the $\boldsymbol{q}$-space convergence of the mass flux. It is the natural, seemingly trivial, generalization of the Cartesian coordinate continuity equation. However, we emphasize that the derivation made no use of $\boldsymbol{x}$-space nor any metric structure. Furthermore, the differential operators are partial derivatives rather than covariant derivatives.

4.3. *Example coordinates*

We consider examples of the mass continuity equation (4.10) to help garner some confidence in its use. First, we trivially recover the Cartesian $\boldsymbol{x}$-space continuity equation by setting $\boldsymbol{q} = \boldsymbol{x}$, $\mathfrak{m} = \rho$, and $\mathcal{M} = 0$ so that

$$\partial_t \rho = -\partial_x(\rho\, \dot{x}) - \partial_y(\rho\, \dot{y}) - \partial_z(\rho\, \dot{z}) = -\boldsymbol{\nabla} \cdot (\rho\, \boldsymbol{v}), \tag{4.12}$$

with $\boldsymbol{v} = \dot{\boldsymbol{x}}$ the velocity of a fluid particle in $\boldsymbol{x}$-space.

Consider next the case of generalized vertical coordinates as introduced by Starr (1945) and used in many ocean models (e.g., Griffies *et al.* 2020). In this case, $\boldsymbol{q} = (x, y, \sigma)$, where $\sigma = \sigma(x, y, z, t)$ is a vertical coordinate such as the hydrostatic pressure, potential density, or a variety of hybrid options. It is common to insist that all generalized vertical coordinates satisfy the constraint that the Jacobian of transformation between $\boldsymbol{x}$-space and generalized vertical coordinates,

$$\mathcal{J} = \frac{\partial z}{\partial \sigma}, \tag{4.13}$$

also known as the specific thickness, is strictly non-zero and single-signed. This assumption ensures that there is a 1-to-1 and invertible relation between σ and z for any (x, y, t). In this case the continuity equation is

$$\partial_t \mathfrak{m} = -\partial_x(\mathfrak{m}\, \dot{x}) - \partial_y(\mathfrak{m}\, \dot{y}) - \partial_\sigma(\mathfrak{m}\, \dot{\sigma}), \tag{4.14}$$

with the mass density given by

$$\mathfrak{m} = \rho\, |\mathcal{J}| = \rho \left| \frac{\partial z}{\partial \sigma} \right|. \tag{4.15}$$

For a Boussinesq fluid, ρ is set to a constant reference value within the mass and tracer continuity equations, in which case the continuity equation (4.14) becomes an equation for the specific thickness (e.g., equation (37) in Young (2012))

$$\partial_t \mathcal{J} = -\partial_x(\mathcal{J}\, \dot{x}) - \partial_y(\mathcal{J}\, \dot{y}) - \partial_\sigma(\mathcal{J}\, \dot{\sigma}). \tag{4.16}$$

Now consider the oceanic case with $\boldsymbol{q} = (S, \Theta, p)$, again assuming the function $\mathfrak{q}$ from $\mathcal{Q}$ to $\mathcal{X}$ is bijective. The Jacobian determinant is given by

$$\mathcal{J} = \left[\frac{\partial \boldsymbol{x}}{\partial S} \times \frac{\partial \boldsymbol{x}}{\partial \Theta} \right] \cdot \frac{\partial \boldsymbol{x}}{\partial p}, \tag{4.17}$$

so that the mass density, $\mathfrak{m} = \rho\, |\mathcal{J}|$, is stretched and squeezed according to the distribution of the seawater volume within (S, Θ, p)-space. Accordingly, the continuity equation is

$$\partial_t \mathfrak{m} = -\partial_S(\mathfrak{m}\, \dot{S}) - \partial_\Theta(\mathfrak{m}\, \dot{\Theta}) - \partial_p(\mathfrak{m}\, \dot{p}) + \mathcal{M}. \tag{4.18}$$

Notably, this form of the continuity equation holds even if the function $\mathfrak{q}$ from $\mathcal{X}$ to $\mathcal{Q}$ is not bijective, since we can use the generalized mass density (3.33) and $\boldsymbol{q}$-space linear momentum (3.34).

For the two dimensional fluid property space $\boldsymbol{q} = (S, \Theta)$,

$$\partial_t \mathfrak{m} = -\partial_S(\mathfrak{m}\, \dot{S}) - \partial_\Theta(\mathfrak{m}\, \dot{\Theta}) + \mathcal{M}. \tag{4.19}$$

Here, the function $\mathfrak{q}$ cannot be 1-to-1 between the 2D $\boldsymbol{q}$-space and 3D $\boldsymbol{x}$-space, so we must always use the generalized mass density (3.33) and $\boldsymbol{q}$-space linear momentum (3.34). We can integrate the mass continuity equation (4.19) over a finite region of $\boldsymbol{q}$-space to develop finite volume budgets. Flow from relatively fresh to salty, $\mathfrak{m}\, \dot{S} > 0$, arises from salt inputs, while flows from relatively cold to warmer, $\mathfrak{m}\, \dot{\Theta} > 0$, are driven by heat input. The convergence

of the mass transports renders a time change to the mass density, $\mathfrak{m}$, and hence the mass contained in each cell. In this manner, the mass budget of the volume in $\boldsymbol{x}$-space enclosed by surfaces of constant S and Θ, that are generally quite complex, is simplified into the mass budget of grid cells in $\boldsymbol{q}$-space.

4.4. *Steady circulation in $\boldsymbol{q}$-space*

In the absence of $\boldsymbol{q}$-space mass sources ($\mathcal{M} = 0$) and for a steady state, the continuity equation (4.6) says that the mass transport exterior form has zero spatial exterior derivative

$$\mathrm{d}\mathcal{T} = 0, \tag{4.20}$$

in which case we say that $\mathcal{T}$ is a spatially closed exterior form. If $\boldsymbol{q}$-space is both simply connected (i.e., we can continuously shrink any simple closed curve into a point while remaining in the domain) and orientable and if $N > 1$, then $\mathcal{T}$ being closed implies that $\mathcal{T}$ is also exact. For the $(N-1)$-form $\mathcal{T}$ to be exact means that there exists a globally defined $(N-2)$-form that we call the mass transport streamfunction, ψ, satisfying

$$\mathcal{T} = \mathrm{d}\psi. \tag{4.21}$$

Note that $\mathrm{d}^2\psi = 0$ is equivalent to the vanishing divergence of a curl (see Appendix B.4).

The steady and source-free mass continuity equation (4.10) leads to the $\boldsymbol{q}$-space non-divergence condition for the $\boldsymbol{q}$-space mass flux

$$\boldsymbol{\nabla}_{\boldsymbol{q}} \cdot (\mathfrak{m}\, \dot{\boldsymbol{q}}) = \partial_\alpha (\mathfrak{m}\, \dot{q}^\alpha) = 0. \tag{4.22}$$

In the special case of $N = 1$, the mass transport $\mathcal{T} = \mathfrak{m}\, \dot{q}^1$ is a 0-form (i.e., a function) that is constant. For $N = 2$, the streamfunction ψ is a 0-form defined on the $N = 2$ dimensional $\boldsymbol{q}$-space domain, $\psi(q^1, q^2)$. The streamfunction's exterior derivative is

$$\mathrm{d}\psi = \partial_\alpha \psi\, \mathrm{d}q^\alpha = \mathcal{T} = \mathfrak{m}\, (\dot{q}^1\, \mathrm{d}q^2 - \dot{q}^2\, \mathrm{d}q^1), \tag{4.23}$$

so that

$$\mathfrak{m}\, \dot{q}^\alpha = \epsilon^{\alpha\beta}\, \partial_\beta \psi, \tag{4.24}$$

with $\epsilon^{\alpha\beta}$ the totally anti-symmetric permutation symbol for $N = 2$, and with ψ having physical dimensions of mass per time, M/T. For $N = 3$, where the mass transport 2-form is given by equation (4.1), the streamfunction is a 1-form defined on the $N = 3$ dimensional $\boldsymbol{q}$-space domain, in which

$$\mathcal{T} = \mathrm{d}(\psi_\alpha\, \mathrm{d}q^\alpha). \tag{4.25}$$

Following the steps in Appendix B.4.4 for taking the exterior derivative of a 1-form leads to

$$\mathfrak{m}\, \dot{q}^\alpha = \epsilon^{\alpha\beta\gamma}\, \partial_\beta \psi_\gamma, \tag{4.26}$$

with $\epsilon^{\alpha\beta\gamma}$ the totally anti-symmetric permutation symbol for $N = 3$, and with the streamfunction components, ψ_γ, having physical dimensions of $\mathrm{M}/(\mathrm{T}\, q^\gamma)$. The right hand side of equation (4.25) can be identified with the curl (in tracer space) of a vector streamfunction, namely the (contravariant) vector associated with the (covariant) 1-form ψ (see Appendix B.3 and equation (B 16)).

5. Angular momentum in fluid property space

We here introduce the angular momentum in fluid property space as a new measure for understanding the circulation in $N > 1$ dimensional $\boldsymbol{q}$-space. The use of angular momentum

does not rely on the steady and source-free assumption required for the streamfunction of Section 4.4. For a $\boldsymbol{q}$-space of dimension $N = 2$ and $N = 3$, we define the angular momenta

$$N = 2: \quad L = \epsilon_{\beta\gamma}\, q^\beta\, \dot{q}^\gamma\, \mathfrak{m}\, \mathrm{d}\mathcal{V} \tag{5.1a}$$

$$N = 3: \quad L_\alpha = \epsilon_{\alpha\beta\gamma}\, q^\beta\, \dot{q}^\gamma\, \mathfrak{m}\, \mathrm{d}\mathcal{V}, \tag{5.1b}$$

where $\epsilon_{\beta\gamma}$ and $\epsilon_{\alpha\beta\gamma}$ are permutation symbols that are numerically identical to those written with raised indices in equations (4.24) and (4.26). Angular momentum for higher dimensional $\boldsymbol{q}$-spaces can be defined by adding an index to the permutation symbol. Conversely, angular momentum in $\boldsymbol{q}$-space for $N = 1$ is not defined since motion with $N = 1$ occurs only along the single coordinate axis.

5.1. *Examples and basic properties*

For the case when $\boldsymbol{q} = \boldsymbol{x}$ with $N = 3$ we recover the angular momentum from Cartesian fluid mechanics

$$\boldsymbol{L} = \boldsymbol{x} \times \boldsymbol{p}, \tag{5.2}$$

where $\boldsymbol{p} = \dot{\boldsymbol{x}}\, \rho\, \mathrm{d}V$ is the linear momentum of a fluid element, and $\times$ is the vector cross product from Cartesian vector analysis. For thermodynamic coordinates $(q^1, q^2, q^3) = (S, \Theta, p)$, with $\mathrm{d}\mathcal{V} = \mathrm{d}S \wedge \mathrm{d}\Theta \wedge \mathrm{d}p$, the $\boldsymbol{q}$-space angular momentum has components

$$L_1 = (\Theta\, \dot{p} - p\, \dot{\Theta})\, \mathfrak{m}\, \mathrm{d}\mathcal{V} \tag{5.3a}$$

$$L_2 = (p\, \dot{S} - S\, \dot{p})\, \mathfrak{m}\, \mathrm{d}\mathcal{V} \tag{5.3b}$$

$$L_3 = (S\, \dot{\Theta} - \Theta\, \dot{S})\, \mathfrak{m}\, \mathrm{d}\mathcal{V}. \tag{5.3c}$$

Likewise, the $N = 2$ fluid property space with $(q^1, q^2) = (S, \Theta)$ and $\mathrm{d}\mathcal{V} = \mathrm{d}S \wedge \mathrm{d}\Theta$ has

$$L = (S\, \dot{\Theta} - \Theta\, \dot{S})\, \mathfrak{m}\, \mathrm{d}\mathcal{V}. \tag{5.4}$$

The $\boldsymbol{q}$-space angular momentum satisfies the following properties.

- For each elemental region of fluid property space, the $\boldsymbol{q}$-space angular momentum is built from the mass of the region multiplied by a couplet that measures the local $\boldsymbol{q}$-space rotation. In Figure 8 we illustrate the S/Θ couplet for the $N = 2$ fluid property space angular momentum given by equation (5.4).
- The physical dimensions of the $\boldsymbol{q}$-space angular momentum depend on the dimensions of the $\boldsymbol{q}$-space coordinates, with the different L_α components for the $N = 3$ case generally having distinct dimensions.
- For $N = 3$ the angular momentum satisfies

$$q^\alpha\, L_\alpha = 0, \tag{5.5}$$

which follows since

$$\epsilon_{\alpha\beta\gamma}\, q^\alpha\, q^\beta\, \dot{q}^\gamma = \boldsymbol{q} \cdot (\boldsymbol{q} \times \dot{\boldsymbol{q}}) = 0. \tag{5.6}$$

It is straightforward to also show that

$$\dot{q}^\alpha\, L_\alpha = 0 \quad \text{and} \quad q^\alpha\, \dot{L}_\alpha = 0. \tag{5.7}$$

Each property also holds for the angular momentum of a fluid element in $\boldsymbol{x}$-space.

- The $\boldsymbol{x}$-space angular momentum depends on the location in space about which the angular momentum is computed. This dependence reflects the subjectivity of the choice for origin when defining angular momentum. Correspondingly, a shift in the definition of the $\boldsymbol{q}$-space origin, such as measuring temperature in Kelvin instead of degrees Celsius, changes the value of the $\boldsymbol{q}$-space angular momentum. In Section 5.2, we find that for steady flow, the global integral of the $\boldsymbol{q}$-space angular momentum remains invariant to the choice of origin.

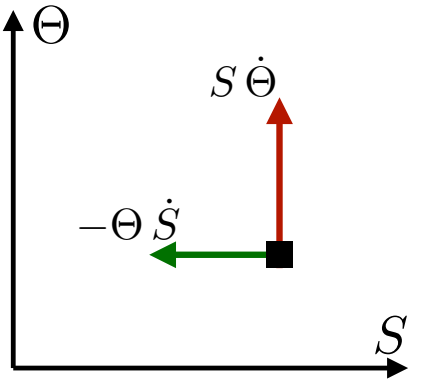

Figure 8: An example of the S/Θ couplet that forms the angular momentum (equation (5.4)) for an elemental region of (S, Θ) fluid property space. The couplet is represented by a horizontal arrow for the $-\Theta\,\dot{S}$ contribution since $\dot{S}$ measures the rate that fluid moves along the S-axis. Likewise, we depict the contribution from $S\,\dot{\Theta}$ as a vertical arrow. For example, with $S > 0$ and $\Theta > 0$, processes that lead to a material increase in Θ (i.e., $\dot{\Theta} > 0$) with an associated decrease in S (i.e., $\dot{S} < 0$) lead to an increase in angular momentum, $L = (S\,\dot{\Theta} - \Theta\,\dot{S})\,\mathfrak{m}\,\mathrm{d}\mathcal{V}$.

5.2. $N = 2$ *with steady and source-free flow*

Consider the case of a steady and source-free flow with an $N = 2$ dimensional fluid property space. In this case, equation (4.24) provides a streamfunction so that the angular momentum is given by

$$L = \epsilon_{\beta\gamma}\, q^\beta\, \dot{q}^\gamma\, \mathfrak{m}\, \mathrm{d}\mathcal{V} \tag{5.8a}$$

$$= \epsilon_{\beta\gamma}\, q^\beta\, \epsilon^{\gamma\zeta}\, \partial_\zeta \psi\, \mathrm{d}\mathcal{V} \tag{5.8b}$$

$$= -(\epsilon_{1\beta}\, \epsilon^{1\zeta} + \epsilon_{2\beta}\, \epsilon^{2\zeta}) q^\beta\, \partial_\zeta \psi\, \mathrm{d}\mathcal{V} \tag{5.8c}$$

$$= -(q^1\, \partial\psi/\partial q^1 + q^2\, \partial\psi/\partial q^2)\, \mathrm{d}\mathcal{V} \tag{5.8d}$$

$$= -\boldsymbol{q} \cdot \boldsymbol{\nabla}_{\boldsymbol{q}} \psi\, \mathrm{d}\mathcal{V} \tag{5.8e}$$

$$= -\boldsymbol{\nabla}_{\boldsymbol{q}} \cdot (\boldsymbol{q}\, \psi)\, \mathrm{d}\mathcal{V} + 2\, \psi\, \mathrm{d}\mathcal{V}, \tag{5.8f}$$

where for the final step we used $\boldsymbol{\nabla}_{\boldsymbol{q}} \cdot \boldsymbol{q} = \partial q^1/\partial q^1 + \partial q^2/\partial q^2 = 2$. Recall from Section 3.5 that the $\boldsymbol{q}$-space boundaries are assumed to be outside the range where fluid exists. Hence, if we integrate the angular momentum (5.8*f*) over all of $\boldsymbol{q}$-space, then the total derivative term drops out since the streamfunction vanishes where there is no fluid. We are thus led to

$$\int L = 2 \int \psi\, \mathrm{d}\mathcal{V}, \tag{5.9}$$

so that in the absence of mass sources, the globally integrated steady state $\boldsymbol{q}$-space angular momentum equals twice the integrated $\boldsymbol{q}$-space mass transport streamfunction. To within an arbitrary sign for the streamfunction, the result (5.9) agrees with the angular momentum computed for a non-divergent depth-integrated ocean using $\boldsymbol{x}$-space coordinates (Holloway & Rhines 1991).

Under a constant shift in the $\boldsymbol{q}$-space coordinates, $\boldsymbol{q} \to \boldsymbol{q} + \boldsymbol{\xi}$ with $\boldsymbol{\xi}$ a constant, the steady state $\boldsymbol{q}$-space angular momentum (5.8*f*) shifts by

$$L \to L - \boldsymbol{\nabla}_{\boldsymbol{q}} \cdot (\boldsymbol{\xi}\, \psi)\, \mathrm{d}\mathcal{V}, \tag{5.10}$$

with the extra term vanishing when integrated globally. Hence, the steady state globally

integrated $\boldsymbol{q}$-space angular momentum remains invariant under a constant shift in the origin of the $\boldsymbol{q}$-space coordinates.

5.3. $N = 3$ *with steady and source-free flow*

We find an analogous result for the $N = 3$ case after a few more manipulations. In this case we make use of the $\boldsymbol{q}$-space streamfunction, ψ_η satisfying $\mathfrak{m}\,\dot{q}^\gamma = \epsilon^{\gamma\zeta\eta}\,\partial_\zeta\psi_\eta$ (equation (4.26)), so that the steady and source-free $\boldsymbol{q}$-space angular momentum is

$$L_\alpha = \epsilon_{\alpha\beta\gamma}\, q^\beta\, \dot{q}^\gamma\, \mathfrak{m}\, \mathrm{d}\mathcal{V} \tag{5.11a}$$

$$= \epsilon_{\gamma\alpha\beta}\, q^\beta\, \epsilon^{\gamma\zeta\eta}\, \partial_\zeta\psi_\eta\, \mathrm{d}\mathcal{V} \tag{5.11b}$$

$$= (\delta^\zeta_\alpha\,\delta^\eta_\beta - \delta^\eta_\alpha\,\delta^\zeta_\beta) q^\beta\, \partial_\zeta\psi_\eta\, \mathrm{d}\mathcal{V} \tag{5.11c}$$

$$= (q^\eta\, \partial_\alpha\psi_\eta - q^\zeta\, \partial_\zeta\psi_\alpha)\, \mathrm{d}\mathcal{V} \tag{5.11d}$$

$$= q^\beta\, (\partial_\alpha\psi_\beta - \partial_\beta\psi_\alpha)\, \mathrm{d}\mathcal{V}, \tag{5.11e}$$

where the third equality made use of the identity between the permutation symbol and Kronecker delta

$$\epsilon_{\gamma\alpha\beta}\,\epsilon^{\gamma\zeta\eta} = \delta^\zeta_\alpha\,\delta^\eta_\beta - \delta^\eta_\alpha\,\delta^\zeta_\beta. \tag{5.12}$$

Moving the derivatives off the streamfunction yields

$$L_\alpha = [\partial_\alpha(q^\beta\,\psi_\beta) - \partial_\beta(q^\beta\,\psi_\alpha) + 2\,\psi_\alpha]\,\mathrm{d}\mathcal{V}, \tag{5.13}$$

where we used equation (2.5). When integrating globally over $\boldsymbol{q}$-space the derivative terms drop out, thus yielding the angular momentum

$$\int L_\alpha = 2\int \psi_\alpha\,\mathrm{d}\mathcal{V}. \tag{5.14}$$

We thus find that for a steady and source-free flow, each component of the integrated $\boldsymbol{q}$-space angular momentum is given by twice the integrated $\boldsymbol{q}$-space streamfunction.

5.4. $\boldsymbol{q}$*-space vs* $\boldsymbol{x}$*-space angular momentum*

As already noted, the $\boldsymbol{q}$-space angular momentum for $N = 3$ is directly analogous to the angular momentum in $\boldsymbol{x}$-space. However, the $\boldsymbol{q}$-space angular momentum is *not* a coordinate transformation of the $\boldsymbol{x}$-space angular momentum. Rather, it is a distinct object that lives in fluid property space and is defined whether or not the function $\mathfrak{q}$ from $\mathcal{X}$ to $\mathcal{Q}$ is bijective. Even so, the $\boldsymbol{q}$-space angular momentum shares certain properties with its $\boldsymbol{x}$-space sibling, with further connections seen when studying tracer angular momentum in Section 7.6.

6. Tracer equation in q-space

To study tracer budgets in fluid property space, we introduce the tracer transport 2-form for $N = 3$

$$\begin{aligned}\mathcal{T}_C = {}& \mathfrak{m}\,(\dot{q}^1\,C + F^1)\,\mathrm{d}q^2\wedge\mathrm{d}q^3 \\ &+ \mathfrak{m}\,(\dot{q}^2\,C + F^2)\,\mathrm{d}q^3\wedge\mathrm{d}q^1 \\ &+ \mathfrak{m}\,(\dot{q}^3\,C + F^3)\,\mathrm{d}q^1\wedge\mathrm{d}q^2,\end{aligned} \tag{6.1}$$

where $\mathfrak{m}\,F^\alpha(\boldsymbol{q},t)$ are components of a subgrid scale flux for tracer concentration, C. If we set C to a constant and assume the subgrid scale flux vanishes with constant C, then the tracer transport in equation (6.1) reduces to the mass transport in equation (4.1). We thus

mathematically interpret the tracer transport just as for the mass transport, only now with the added subgrid contribution.

In regions of $\boldsymbol{x}$-space where the mapping to $\boldsymbol{q}$-space is 1-to-1 (with $N = 3$), we can relate the subgrid scale tracer flux's $\boldsymbol{x}$-space components to its $\boldsymbol{q}$-space components according to the chain-rule coordinate transformation from tensor analysis

$$F^\alpha(\boldsymbol{q}) = \left(\frac{\partial \mathfrak{q}^\alpha}{\partial x^a}\, F^a\right)(\boldsymbol{x}) = \boldsymbol{\nabla} q^\alpha \cdot \boldsymbol{F}(\boldsymbol{x}), \tag{6.2}$$

where $\boldsymbol{x} = \mathfrak{x}(\boldsymbol{q}) = \mathfrak{q}^{-1}(\boldsymbol{q})$, and $\rho\, F^a$ are the Cartesian components of the subgrid scale tracer flux. We also introduced shorthand notation for evaluating a product of functions:

$$(fg)(\boldsymbol{x}) \equiv f(\boldsymbol{x})\, g(\boldsymbol{x}). \tag{6.3}$$

More generally, when the mapping from $\boldsymbol{x}$-space to $\boldsymbol{q}$-space is not 1-to-1 (such as when $N \neq 3$), the components to the subgrid scale tracer flux in $\boldsymbol{q}$-space are found by following the sifting approach from Section 3.4. That is, the generalized subgrid flux in $\boldsymbol{q}$-space is the mass-weighted average of the subgrid flux in $\boldsymbol{x}$-space over regions $\boldsymbol{x} \in \mathcal{X}$ where $\mathfrak{q}(\boldsymbol{x}) = \boldsymbol{q}$,

$$(F^\alpha)^{\text{gen}}(\boldsymbol{q})\; \mathfrak{m}^{\text{gen}}(\boldsymbol{q}) = \int_{\mathcal{X}} \rho(\boldsymbol{x}) \left(\frac{\partial \mathfrak{q}^\alpha}{\partial x^a}\, F^a\right)(\boldsymbol{x})\, \delta_{\boldsymbol{q}}\big(\mathfrak{q}(\boldsymbol{x})\big)\, \mathrm{d}V. \tag{6.4}$$

As noted at the end of Section 3.4, in the subsequent development we drop the "gen" notation for brevity.

Following the same manipulations as used in Section 4.2 for the mass continuity equation leads to the tracer continuity equation in $\boldsymbol{q}$-space

$$\partial_t(\mathfrak{m}\, C) = -\partial_\alpha(\mathfrak{m}\, C\, \dot{q}^\alpha + \mathfrak{m}\, F^\alpha) + \mathfrak{m}\, \mathcal{S}_{\text{pure}} + \mathcal{M}\, C_{\text{input}}. \tag{6.5}$$

We introduced a tracer source, $\mathcal{S}_{\text{pure}}$, with physical dimensions of tracer concentration per time, along with a source, $\mathcal{M}\, C_{\text{input}}$, arising from the tracer contained in the mass source. Radiation is an example tracer source, $\mathcal{S}_{\text{pure}}$, that is independent of the mass source. Making use of the mass continuity equation (4.10) yields the advective expression of the tracer equation

$$(\partial_t + \dot{q}^\alpha\, \partial_\alpha)\, C = -\mathfrak{m}^{-1}\, \partial_\alpha(\mathfrak{m}\, F^\alpha) + \mathcal{S}, \tag{6.6}$$

where the combined tracer source is given by

$$\mathfrak{m}\, \mathcal{S} = \mathfrak{m}\, \mathcal{S}_{\text{pure}} + \mathcal{M}\, (C_{\text{input}} - C). \tag{6.7}$$

Notice that if the tracer concentration associated with the input mass source equals to the ambient tracer concentration, then $\mathfrak{m}\, \mathcal{S} = \mathfrak{m}\, \mathcal{S}_{\text{pure}}$. Also note that setting the tracer concentration to a constant reduces the tracer equation (6.5) to the corresponding flux form of mass conservation given by equation (4.10).

The convergence of the subgrid scale tracer flux found in equation (6.6) is given by

$$\mathcal{D} \equiv -\mathfrak{m}^{-1}\, \partial_\alpha(\mathfrak{m}\, F^\alpha). \tag{6.8}$$

When the subgrid scale flux is given in the downgradient diffusive form, as in Section 7.2 ahead, then $\mathcal{D}$ is a generalized Laplacian operator applied to the tracer C. In Appendix A we offer examples of this operator.

7. Fluid property space as tracer space

We now study the case where fluid property space is defined by N tracer coordinates,

$$\boldsymbol{q} = \boldsymbol{C} = (C^1, \ldots, C^N) \Longleftrightarrow q^\alpha = C^\alpha \quad \alpha = 1, \ldots, N, \tag{7.1}$$

with the Jacobian and mass density

$$\mathcal{J} = \frac{\partial \boldsymbol{x}}{\partial \boldsymbol{C}} \quad \text{and} \quad \mathfrak{m} = \rho \, |\mathcal{J}| \tag{7.2}$$

and the mass continuity equation (4.10)

$$\partial_t \mathfrak{m} = -\partial_\alpha (\mathfrak{m} \, \dot{C}^\alpha) + \mathcal{M}. \tag{7.3}$$

Recall that if the function $\mathfrak{q}$ from $\mathcal{X}$ to $\mathcal{Q}$ is not bijective, as when $N \neq 3$, then we can patch regions together by following the methods from Section 3.4. Thus, we make use of the generalized Jacobian from equation (3.20) when $N = 3$, or when N is arbitrary we use equation (3.24) in the discrete case and equation (3.31) in the continuous case.

7.1. *The tracer equation*

With $\boldsymbol{q} = \boldsymbol{C}$, the tracer equation (6.6) becomes

$$\mathfrak{m} \, (\partial_t + \dot{C}^\alpha \, \partial_\alpha) \, C^\beta = -\partial_\alpha (\mathfrak{m} \, F^{\alpha\beta}) + \mathfrak{m} \, \mathcal{S}^\beta, \tag{7.4}$$

where $\mathfrak{m} \, F^{\alpha\beta}$ is the α-th component of the subgrid flux for tracer C^β, and $\mathcal{S}^\beta$ is the source for tracer C^β. Since tracers now act as coordinates, the tracer equation (7.4) simplifies to

$$\mathfrak{m} \, \dot{C}^\beta = -\partial_\alpha (\mathfrak{m} \, F^{\alpha\beta}) + \mathfrak{m} \, \mathcal{S}^\beta, \tag{7.5}$$

which follows since the partial time derivative, ∂_t, is computed holding each of the tracer coordinates fixed ($\partial_t C^\alpha = 0$), and since $\partial_\alpha \, C^\beta = \delta^\beta_\alpha$ (see equation (2.5)).

If $\mathfrak{q}$ is bijective, then $F^{\alpha\beta}(\boldsymbol{q})$ is given similarly to $F^\alpha(\boldsymbol{q})$ in (6.2) but with $\rho \boldsymbol{F}$ replaced by $\rho \boldsymbol{F}^\beta$, the subgrid flux for tracer C^β; otherwise we use the generalized form $(F^{\alpha\beta})^{\text{gen}}(\boldsymbol{q})$ which is similarly modified from the expression for $(F^\alpha)^{\text{gen}}(\boldsymbol{q})$ in equation (6.4).

7.2. *Subgrid scale tracer flux*

We suppose a flux-gradient relation for the subgrid tracer flux by introducing a kinematic diffusion tensor, $\boldsymbol{K}$, which is a symmetric and positive definite second order tensor. We also assume that all tracers are diffused by the same diffusion tensor. The latter assumption is valid if all mixing is ultimately achieved by vigorous small scale isotropic turbulence (e.g., Davis 1994; Gregg *et al.* 2018), whereby the turbulent diffusivity is equal for all tracers (see in particular Sections 2.5, 8.5, and Figure 14 from Gregg *et al.* (2018)). However, if the turbulence is weak or absent and molecular diffusion is a relatively large contributor to tracer mixing, then tracers with different molecular diffusivities can have different effective diffusivities. For example, the molecular thermal diffusivity in seawater is roughly 100 times larger than the salt diffusivity (Gill 1982). This leads to double-diffusive convection in quiescent ocean regions yielding larger effective diffusivities for temperature than salt (Schmitt 1994).

An anti-symmetric component to the mixing tensor is often included in numerical ocean models (Griffies 1998, 2004; Groeskamp *et al.* 2019). This skew-diffusion is aimed at parameterizing stirring processes not captured by a model's resolved flow (see Section 2.3 of Groeskamp *et al.* (2019)). We here focus on mixing parameterized by a symmetric diffusion tensor since it directly leads to transport across tracer surfaces (which oceanographers refer to as "water mass transformation"), whereas the anti-symmetric skew diffusion tensor is equivalent to an advection.

Representing the subgrid flux for tracer C^β in terms of its $\boldsymbol{x}$-space coordinates yields

$$F^{a\beta} = -\mathbb{K}^{ab} \, \partial_b C^\beta, \tag{7.6}$$

where $\mathbb{K}^{ab}$ is the $\boldsymbol{x}$-space representation of the diffusion tensor $\boldsymbol{K}$ that has dimensions $L^2\,T^{-1}$.

If $\mathfrak{q}$ is bijective, the diffusion tensor can be represented in tracer coordinates through the coordinate transformation

$$\mathbb{K}^{\alpha\beta}(\boldsymbol{q}) = \Big(\partial_a C^\alpha\, \mathbb{K}^{ab}\, \partial_b C^\beta\Big)(\boldsymbol{x}) = \Big(\boldsymbol{\nabla} C^\alpha \cdot \boldsymbol{K} \cdot \boldsymbol{\nabla} C^\beta\Big)(\boldsymbol{x}), \tag{7.7}$$

where $\boldsymbol{x} = \mathfrak{x}(\boldsymbol{q}) = \mathfrak{q}^{-1}(\boldsymbol{q})$ as in equation (6.2). The tracer coordinate representation of the subgrid flux then satisfies

$$\mathfrak{m}\, F^{\beta\alpha} = -\mathfrak{m}\, \mathbb{K}^{\alpha\beta} = \mathfrak{m}\, F^{\alpha\beta} \tag{7.8}$$

by applying equations (7.6) and (7.7) to the coordinate transformation equation (6.2), and using the symmetry of $\mathbb{K}^{ab}$ and hence $\mathbb{K}^{\alpha\beta}$ for the last equality. We thus see that the tracer space representation of the subgrid flux tensor is minus the tracer space representation of the diffusion tensor. Note again that this identity (and the symmetry of $\mathbb{K}^{\alpha\beta}$) requires that the same diffusion tensor applies to each tracer.

If $\mathfrak{q}$ is not bijective, we substitute equation (7.6) into the expression (6.4) for $(F^{\alpha\beta})^{\text{gen}}(\boldsymbol{q})$ to give

$$(F^{\alpha\beta})^{\text{gen}}(\boldsymbol{q})\, \mathfrak{m}^{\text{gen}}(\boldsymbol{q}) = \int_{\mathcal{X}} \rho(\boldsymbol{x})\, \Big(\partial_a C^\alpha\, F^{a\beta}\Big)(\boldsymbol{x})\, \delta_{\boldsymbol{q}}\big(\mathfrak{q}(\boldsymbol{x})\big)\, \mathrm{d}V \tag{7.9a}$$

$$= -\int_{\mathcal{X}} \rho(\boldsymbol{x})\, \Big(\boldsymbol{\nabla} C^\alpha \cdot \boldsymbol{K} \cdot \boldsymbol{\nabla} C^\beta\Big)(\boldsymbol{x})\, \delta_{\boldsymbol{q}}\big(\mathfrak{q}(\boldsymbol{x})\big)\, \mathrm{d}V \tag{7.9b}$$

We define the generalized diffusion tensor, $(\mathbb{K}^{\alpha\beta})^{\text{gen}}$, as a mass-weighted mean of $\boldsymbol{\nabla} C^\alpha \cdot \boldsymbol{K} \cdot \boldsymbol{\nabla} C^\beta$ evaluated at points $\boldsymbol{x} \in \mathcal{X}$ where $\mathfrak{q}(\boldsymbol{x}) = \boldsymbol{q}$:

$$(\mathbb{K}^{\alpha\beta})^{\text{gen}}(\boldsymbol{q})\, \mathfrak{m}^{\text{gen}}(\boldsymbol{q}) = \int_{\mathcal{X}} \rho(\boldsymbol{x})\, \Big(\boldsymbol{\nabla} C^\alpha \cdot \boldsymbol{K} \cdot \boldsymbol{\nabla} C^\beta\Big)(\boldsymbol{x})\, \delta_{\boldsymbol{q}}\big(\mathfrak{q}(\boldsymbol{x})\big)\, \mathrm{d}V. \tag{7.10}$$

Comparing equations (7.9*b*) and (7.10) shows that $(F^{\alpha\beta})^{\text{gen}}$ and $(\mathbb{K}^{\alpha\beta})^{\text{gen}}$ still obey equation (7.8) and are symmetric, as long as all tracers are diffused by the same, symmetric, $\boldsymbol{K}$. Therefore, in the following we again drop the "gen" notation and use the simpler expressions (7.5) and (7.8).

The corresponding representation of the diffusion operator, equation (6.8), acting on tracer C^β is given by

$$-\,\mathfrak{m}^{-1}\, \partial_\alpha(\mathfrak{m}\, F^{\alpha\beta}) = \mathfrak{m}^{-1}\, \partial_\alpha(\mathfrak{m}\, \mathbb{K}^{\alpha\beta}). \tag{7.11}$$

Note that these relations were also used by Mackay *et al.* (2018, 2020) in an oceanographic inverse study.

7.3. *Variances and covariances for $\boldsymbol{q} = (S, \Theta)$ without sources*

Consider the tracer equation (7.5) for the $N = 2$ tracer space with $\boldsymbol{q} = (S, \Theta)$ as an oceanic example, and suppose there are no tracer sources (whether interior or boundary). The two tracer equations are

$$\mathfrak{m}\, \dot{S} = -\partial_S(\mathfrak{m}\, F^{SS}) - \partial_\Theta(\mathfrak{m}\, F^{\Theta S}), \tag{7.12a}$$

$$\mathfrak{m}\, \dot{\Theta} = -\partial_S(\mathfrak{m}\, F^{S\Theta}) - \partial_\Theta(\mathfrak{m}\, F^{\Theta\Theta}). \tag{7.12b}$$

For the salinity equation, its two flux components, $\mathfrak{m}\, F^{\alpha S}$, include F^{SS}, arising from the subgrid flux of S in the S direction, and $F^{\Theta S}$, arising from the subgrid flux of S in the Θ direction. The Θ equation has similar flux components.

We expose some properties of the subgrid flux components by studying how they affect the evolution of tracer variance (squared tracer) and tracer covariance (product of two different

tracers) (see Ruan & Ferrari (2021) for an analogous discussion). Start by considering the evolution equation for one-half the squared salinity, which is readily derived from the salinity equation (7.12*a*),

$$\mathfrak{m}\, S\, \dot{S} = -\partial_\alpha(\mathfrak{m}\, S\, F^{\alpha S}) + \mathfrak{m}\, F^{SS}, \tag{7.13}$$

where $S\,\dot{S} = \frac{1}{2}\mathrm{D}(S^2)/\mathrm{D}t$ is half the mass-weighted material evolution of the squared salinity, and we used $\partial_\alpha C^\beta = \delta^\beta_\alpha$ from equation (2.5). The first term on the RHS of (7.13) is a flux-convergence term that represents the redistribution of variance. Its global integral vanishes as both the mass density and the subgrid flux vanish outside the regions of $\boldsymbol{q}$-space where seawater exists. The second term is given by (7.9*a*) and (7.9*b*) as

$$\mathfrak{m}\, F^{SS} = \int_{\mathcal{X}} \rho(\boldsymbol{x}) \, \Big(\boldsymbol{\nabla} S \cdot \boldsymbol{F}^S\Big)(\boldsymbol{x}) \, \delta_{\boldsymbol{q}}\big(\mathfrak{q}(\boldsymbol{x})\big) \, \mathrm{d}V \tag{7.14a}$$

$$= -\int_{\mathcal{X}} \rho(\boldsymbol{x}) \, (\boldsymbol{\nabla} S \cdot \boldsymbol{K} \cdot \boldsymbol{\nabla} S)(\boldsymbol{x}) \, \delta_{\boldsymbol{q}}\big(\mathfrak{q}(\boldsymbol{x})\big) \, \mathrm{d}V \leqslant 0, \tag{7.14b}$$

where the inequality follows for downgradient fluxes in which $\mathbb{K}$ is a symmetric and positive definite diffusion tensor. Hence, in the presence of diffusion, the integral of $\mathfrak{m}\, F^{SS}\, \mathrm{d}\mathcal{V}$ over a finite region of $\boldsymbol{q}$-space provides a sign-definite sink to the evolution of the squared salinity, and hence a sink to salinity variance.

Equation (7.14*b*) is reminiscent of the formula (7a) in Winters & D'Asaro (1996) for the flux of a scalar θ across an isosurface of θ per unit horizontal area:

$$\phi_d(\theta) = -\kappa \, \frac{\mathrm{d}z^*}{\mathrm{d}\theta} \, \langle (\boldsymbol{\nabla}\theta)^2 \rangle_\theta, \tag{7.15}$$

where z^* is the mean height of the θ surface, and in our notation $\phi_d = F^{\theta\theta}$, κ is the (isotropic) diffusivity (i.e. $\mathbb{K}^{ab} = \kappa \delta^{ab}$), and $\langle (\boldsymbol{\nabla}\theta)^2 \rangle_\theta$ represents the thickness-weighted average of $(\boldsymbol{\nabla}\theta)^2$ on the θ surface. In our formalism, $\mathrm{d}z^*/\mathrm{d}\theta$, the volume per unit area per unit θ, represents the generalized Jacobian $\mathrm{d}V/\mathrm{d}\mathcal{V}$ for the transformation from the $N = 3$ fluid property space (x, y, θ) back to $\boldsymbol{x}$-space. Both equations (7.14*b*) and (7.15) emphasize how the flux across a scalar surface is increased by folding and break-up of the surface.

Following similar methods, we readily obtain an evolution equation for the product of $S\,\Theta$ from equations (7.12*a*) and (7.12*b*), whereby

$$\mathfrak{m}\, \Theta\, \dot{S} = -\partial_\alpha(\mathfrak{m}\, \Theta\, F^{\alpha S}) + \mathfrak{m}\, F^{\Theta S} \tag{7.16a}$$

$$\mathfrak{m}\, S\, \dot{\Theta} = -\partial_\alpha(\mathfrak{m}\, S\, F^{\alpha \Theta}) + \mathfrak{m}\, F^{S\Theta}. \tag{7.16b}$$

The sum $\Theta\,\dot{S} + S\,\dot{\Theta}$ measures changes to the (S, Θ)-covariance when integrated over the fluid domain. Since S and Θ are assumed to be diffused by the same symmetric tensor, with

$$\boldsymbol{F}^S \cdot \boldsymbol{\nabla}\Theta = -\boldsymbol{\nabla}\Theta \cdot \boldsymbol{K} \cdot \boldsymbol{\nabla} S = \boldsymbol{F}^\Theta \cdot \boldsymbol{\nabla} S, \tag{7.17}$$

it follows that the S component of the subgrid-scale flux of Θ is equal to the Θ component of the subgrid-scale flux of S:

$$\mathfrak{m}\, F^{S\Theta} = \int_{\mathcal{X}} \rho(\boldsymbol{x}) \, \Big(\boldsymbol{\nabla} S \cdot \boldsymbol{F}^\Theta\Big)(\boldsymbol{x}) \, \delta_{\boldsymbol{q}}\big(\mathfrak{q}(\boldsymbol{x})\big) \, \mathrm{d}V \tag{7.18a}$$

$$= \int_{\mathcal{X}} \rho(\boldsymbol{x}) \, \Big(\boldsymbol{\nabla}\Theta \cdot \boldsymbol{F}^S\Big)(\boldsymbol{x}) \, \delta_{\boldsymbol{q}}\big(\mathfrak{q}(\boldsymbol{x})\big) \, \mathrm{d}V \tag{7.18b}$$

$$= \mathfrak{m}\, F^{\Theta S}. \tag{7.18c}$$

Hence, a salinity flux crossing temperature surfaces causes an evolution of (S, Θ)-covariance,

as does a temperature flux crossing salinity surfaces. Since these two fluxes, $F^{\Theta S}$ and $F^{S\Theta}$, are not sign-definite, the globally integrated $S\,\Theta$ (and hence the (S,Θ)-covariance) can increase or decrease in time, in contrast to the globally integrated squared tracer (and hence tracer variance) which decreases in time.

To summarise, if we measure variance loss in a tracer mixing experiment, diffusive fluxes of salinity are directed down the salinity gradient and diffusive fluxes of temperature are directed down the temperature gradient. In contrast, measured variance gain corresponds to fluxes up the gradient. Measured covariance sources and sinks (sign unclear) reflect diffusive fluxes of salinity that project onto the temperature gradient and fluxes of temperature that project onto the salinity gradient.

7.4. *Mass conservation*

Making use of the tracer equation in the form (7.5) allows us to write the mass continuity equation (7.3) as

$$\partial_t \mathfrak{m} = -\partial_\alpha \left[\partial_\beta(\mathfrak{m}\,\mathbb{K}^{\alpha\beta}) + \mathfrak{m}\,\mathcal{S}^\alpha\right] + \mathcal{M}. \tag{7.19}$$

This equation locally connects the evolution of mass within tracer space to the mixing of tracers that acts to move mass across the tracer contours, plus any contributions from tracer and mass sources.

7.5. *Tracer coordinate streamfunction*

Now consider a steady tracer space circulation with zero mass source ($\mathcal{M} = 0$), in which case the mass continuity equation (7.19) reduces to the non-divergence condition

$$0 = -\partial_\alpha[\partial_\beta(\mathfrak{m}\,\mathbb{K}^{\alpha\beta}) + \mathfrak{m}\,\mathcal{S}^\alpha] = \partial_\alpha(\mathfrak{m}\,\dot{C}^\alpha), \tag{7.20}$$

having used the tracer equation (7.5) and the subgrid tracer flux (7.8) for the second equality. Connecting to the $N = 3$ streamfunction in equation (4.26), and again using (7.5), leads to

$$\mathfrak{m}\,\dot{C}^\alpha = \epsilon^{\alpha\beta\gamma}\,\partial_\beta\psi_\gamma = \partial_\beta(\mathfrak{m}\,\mathbb{K}^{\alpha\beta}) + \mathfrak{m}\,\mathcal{S}^\alpha. \tag{7.21}$$

We recognise the term $\epsilon^{\alpha\beta\gamma}\,\partial_\beta\psi_\gamma$ as the tracer-space curl of the vector streamfunction (as discussed after equation (4.26)) and the term $\partial_\beta(\mathfrak{m}\,\mathbb{K}^{\alpha\beta})$ as, using equation (7.8), the tracer-space convergence of the subgrid scale flux of tracer C^α.

Equation (7.21) reveals that the streamfunction for steady circulation in tracer space is locally related to the diffusion tensor and to the $\boldsymbol{q}$-space tracer sources. This connection follows since tracer mixing, as parameterized by a symmetric diffusion tensor, generates local circulation in tracer space. Also, recall that $\boldsymbol{q}$-space tracer sources reflect the usual $\boldsymbol{x}$-space sources (e.g., biogeochemical sources) as well as $\boldsymbol{x}$-space boundary fluxes. In the absence of any $\boldsymbol{q}$-space tracer sources (including zero $\boldsymbol{x}$-space boundary fluxes), then diffusion leads to a steady state with homogenized tracers and thus to a trivial (zero) $\boldsymbol{q}$-space circulation where $\dot{\boldsymbol{C}} = 0$.

7.6. *Tracer angular momentum*

When using tracer coordinates, we refer to the $\boldsymbol{q}$-space angular momentum as the tracer angular momentum, which takes the form

$$L_\alpha = \epsilon_{\alpha\beta\gamma}\,C^\beta\,\dot{C}^\gamma\,\mathfrak{m}\,\mathrm{d}\mathcal{V} \tag{7.22a}$$

$$= \epsilon_{\alpha\beta\gamma}\,C^\beta\left[-\partial_\zeta(\mathfrak{m}\,F^{\zeta\gamma}) + \mathfrak{m}\,\mathcal{S}^\gamma\right]\mathrm{d}\mathcal{V} \tag{7.22b}$$

$$= \epsilon_{\alpha\beta\gamma}\left[-\partial_\zeta(\mathfrak{m}\,F^{\zeta\gamma}\,C^\beta) + \mathfrak{m}\,\mathcal{S}^\gamma\,C^\beta\right]\mathrm{d}\mathcal{V}. \tag{7.22c}$$

For the final step we made use of the identity

$$\epsilon_{\alpha\beta\gamma}\,\partial_\zeta C^\beta\,F^{\zeta\gamma} = \epsilon_{\alpha\beta\gamma}\,\delta^\beta_\zeta\,F^{\zeta\gamma} = \epsilon_{\alpha\beta\gamma}\,F^{\beta\gamma} = 0, \tag{7.23}$$

which follows from anti-symmetry of $\epsilon_{\alpha\beta\gamma}$ along with symmetry of $F^{\beta\gamma}$ (see equation (7.8)). The identity (7.23) is a critical step that allows us to write each component of the tracer angular momentum in equation (7.22*c*) as a tracer space convergence plus a source. Hence, integrating over all of tracer space removes contributions from interior diffusive mixing processes, leaving just tracer sources

$$\int L_\alpha = \epsilon_{\alpha\beta\gamma}\int \mathcal{S}^\gamma\,C^\beta\,\mathfrak{m}\,\mathrm{d}\mathcal{V}. \tag{7.24}$$

Recall that tracer sources in $\boldsymbol{q}$-space correspond to both the $\boldsymbol{x}$-space sources plus $\boldsymbol{x}$-space boundary fluxes. It follows that the global integral for each of the three components to the tracer angular momentum is identically zero when the $\boldsymbol{q}$-space source for the complementary tracers vanish

$$\int L_\alpha = 0 \quad \text{if } \mathcal{S}^\gamma = 0 \text{ for all } \gamma \neq \alpha. \tag{7.25}$$

7.7. *Tracer angular momentum in $\boldsymbol{x}$-space*

We can realize the above result for the tracer angular momentum by integrating over $\boldsymbol{x}$-space rather than tracer space, where Cartesian coordinates leads to

$$L_\alpha = \epsilon_{\alpha\beta\gamma}\,C^\beta\,[-\boldsymbol{\nabla}\cdot(\rho\,\boldsymbol{F}^\gamma) + \rho\,\mathcal{S}^\gamma]\,\mathrm{d}V \tag{7.26a}$$

$$= \epsilon_{\alpha\beta\gamma}\left[-\boldsymbol{\nabla}\cdot(C^\beta\,\rho\,\boldsymbol{F}^\gamma) + \rho\,C^\beta\,\mathcal{S}^\gamma\right]\mathrm{d}V, \tag{7.26b}$$

where we used the identity

$$\epsilon_{\alpha\beta\gamma}\,\boldsymbol{\nabla}C^\beta\cdot\boldsymbol{F}^\gamma = -\epsilon_{\alpha\beta\gamma}\,\boldsymbol{\nabla}C^\beta\cdot\boldsymbol{K}\cdot\boldsymbol{\nabla}C^\gamma = 0. \tag{7.27}$$

We again see that the global integral of the tracer angular momentum reduces to contributions from $\boldsymbol{x}$-space sources plus $\boldsymbol{x}$-space boundary fluxes.

7.8. *Why diffusion plays no role in global integrated tracer angular momentum*

It is remarkable that diffusive mixing cannot engender any globally integrated tracer angular momentum. This null result holds so long as the diffusion tensor is symmetric and the same diffusion tensor is used for each pair of tracers building the angular momentum. Diffusion tensor symmetry ensures that the contribution from diffusion to angular momentum couplets (Figure 8) precisely balance when integrated over the domain. Mathematically, this balance manifests since the local contribution from the diffusive flux appears inside of a total derivative operator.

There is precedent for this result from studying the $\boldsymbol{x}$-space angular momentum. For a Newtonian fluid, the stress tensor is symmetric, which means that stresses do not alter the angular momentum integrated over the fluid interior (see, for example, Section 17.3.3 of Griffies (2004) or Section 2.3.1 of Olbers *et al.* (2012)). Likewise, we here find that a single symmetric diffusion tensor used for all tracers cannot alter the globally integrated tracer angular momentum. If, furthermore, there are no $\boldsymbol{x}$-space boundary contributions or $\boldsymbol{x}$-space sources, then the integrated tracer angular momentum is zero. Conversely, if we diagnose that the integrated tracer angular momentum is nonzero, then we conclude that either (i) boundary effects or (ii) sources are at play, or that (iii) different tracers have different diffusion tensors. In particular, if two of the tracers are Θ and S and if there are no boundary contributions or sources, then a nonzero integrated tracer angular momentum is a signature of double

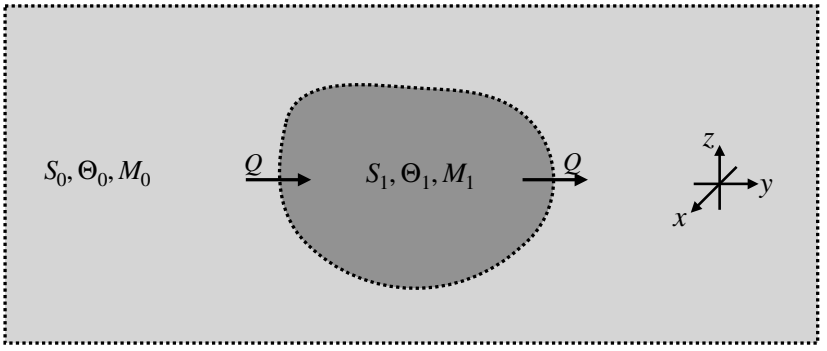

Figure 9: An isolated region of fluid exposed to mass and tracer transport with the surrounding fluid. Here we consider the case of $\boldsymbol{q} = (S, \Theta, C)$ and focus on the tracer angular momentum component $L = (S\,\dot{\Theta} - \Theta\,\dot{S})\,\mathfrak{m}\,d\mathcal{V}$, with C an arbitrary passive tracer. The dark region has uniform (S_1, Θ_1) and fixed mass, M_1, whereas the surrounding fluid has uniform (S_0, Θ_0) and fixed mass, M_0. Fluid moves relative to the dark region with a mass transport, $Q > 0$. Mass does not converge anywhere in the fluid, including the dark region.

diffusive processes, in which the diffusivities (either molecular or turbulent) of Θ and S are distinct.

7.9. *Tracer angular momentum in an exchange model*

Consider a discrete exchange model for mixing that complements our previous examination of continuous diffusion. In Figure 9 we depict an isolated region with fixed mass M_1 and uniform (S_1, Θ_1), surrounded by fluid with fixed mass M_0 and uniform (S_0, Θ_0). A mass transport, $Q > 0$ (dimensions mass per time), carries fluid through the region, and mass does not converge anywhere. We model the exchange of fluid properties between the small region and large region via upwind exchange, as commonly used for transport in box models such as Stommel (1961).

The above assumptions lead to the (S, Θ) evolution equations

$$M_0\,\dot{S}_0 = -Q\,(S_0 - S_1) \qquad M_0\,\dot{\Theta}_0 = -Q\,(\Theta_0 - \Theta_1) \tag{7.28a}$$

$$M_1\,\dot{S}_1 = Q\,(S_0 - S_1) \qquad M_1\,\dot{\Theta}_1 = Q\,(\Theta_0 - \Theta_1), \tag{7.28b}$$

which manifest the conservation of salt and enthalpy for the fixed mass system. The corresponding thermohaline angular momentum component, $L = (S\,\dot{\Theta} - \Theta\,\dot{S})\,\mathfrak{m}\,d\mathcal{V}$, for each region is given by

$$L_0 = [S_0\,\dot{\Theta}_0 - \dot{S}_0\,\Theta_0]\,M_0 \tag{7.29a}$$

$$L_1 = [S_1\,\dot{\Theta}_1 - \dot{S}_1\,\Theta_1]\,M_1. \tag{7.29b}$$

Using the upwind time tendencies (7.28*a*)–(7.28*b*) renders a vanishing net thermohaline angular momentum,

$$L_0 + L_1 = 0. \tag{7.30}$$

We thus find a precise cancellation of the thermohaline angular momentum generated by the upwind transport through the two regions. This example offers yet another manifestation of how mixing, whether diffusive mixing or exchange mixing, leads to a zero net tracer angular momentum so long as the mixing acts the same for each tracer.

7.10. *Connection to probability angular momentum*

Weiss *et al.* (2019) made use of a probability angular momentum to characterize non-equilibrium steady states found on the fluid property space defined by climate indices. In formulating their angular momentum, they made use of a Fokker-Planck equation for the probability density function, and considered both drift and diffusion in this equation. Our approach focuses on the tracer equation rather than the Fokker-Planck equation, though the two are related (e.g., see Section 2.5.2 of van Sebille *et al.* 2018). Furthermore, we considered both time-dependent and steady flows. Developing insights into the connection between the two angular momenta is worthy of further research.

8. Summary and conclusions

In this paper we have developed a mathematical formalism for the mechanics of fluid flow in an arbitrary fluid property space ($\boldsymbol{q}$-space) as defined by any number of continuous properties. Since $\boldsymbol{q}$-space generally has no metric, we made use of some rudimentary features of exterior forms (also known as differential forms; see Appendix B) in the derivation of $\boldsymbol{q}$-space , tracer conservation, steady state streamfunction, and angular momentum. By pursuing the formulation within fluid property space defined by continuous properties, we were able to develop the mechanics of circulation in $\boldsymbol{q}$-space. Although the mapping from $\boldsymbol{x}$-space to $\boldsymbol{q}$-space is not generally a 1-to-1 coordinate transformation, we have detailed a method that gives the same budget equations even when this mapping is many-to-1. This approach has allowed us to expose the underlying mathematical structure of the budget equations and to seamlessly make connections to special cases when the mapping from $\boldsymbol{x}$-space to $\boldsymbol{q}$-space is 1-to-1.

We offered a case study of a fluid property space defined by tracers. Working in this space reveals a local connection between tracer mixing and circulation in tracer space. That connection is highly constrained when the mixing is parameterized by a single symmetric diffusion tensor, in which case we find that the global integral of the tracer angular momentum is unaffected by diffusive mixing, with this property holding for both steady and time evolving flows. We thus find that although diffusive mixing (along with boundary transport and sources) plays a key role in local fluid motion across tracer surfaces (what oceanographers term water mass transformation), and the local behaviour of tracer angular momentum, only boundary transport and interior sources can alter the globally integrated tracer angular momentum. Consequently, any net tracer angular momentum signals the role of tracer sources or boundary processes, or that mixing of different tracers occurs via different diffusion tensors (e.g., double diffusive processes).

We have revealed fundamental constraints on fluid circulation in a general fluid property space and developed mathematical foundations for further advances. We propose that these constraints will be of practical use in observational and numerical model-based descriptions of mean circulation (e.g. Groeskamp *et al.* 2017), its variability (e.g. Evans *et al.* 2014, 2018), its response to forcing such as experienced by the ocean from global warming (e.g. Zika *et al.* 2021; Sohail *et al.* 2022), and potentially to other sub-fields of fluid mechanics (e.g. Laliberté *et al.* 2015). We are motivated to pursue such lines of research and hope this study motivates others as well.

Acknowledgements. We thank the following colleagues for suggestions made at various points of this research: Rebecca Beadling, Henri Drake, Baylor Fox-Kemper, Graeme MacGilchrist, Trevor McDougall, Alberto Naveira Garabato, Charles Nurser, Chris Wilson, and Houssam Yassin.

Funding. This work was supported by the UK NERC project Transient tracer-based Investigation of

Circulation and Thermal Ocean Change (TICTOC) (A.J.G.N., grant number NE/P019293/1), and the Australian Research Council (G.J.S., grant number FL150100090).

Declaration of interests. The authors report no conflict of interest.

Data availability statement. For Figure 1, we made use of the ACCESS-CM2 climate model of Bi *et al.* (2020), specifically years 490-499 of the pre-industrial simulation. The circulation makes use of the 3D non-divergent velocity as well as sub-grid scale transport and the local tendency as recommended by Groeskamp *et al.* (2014). These ACCESS-CM2 data will be made freely available via figshare.com at time of publication. For Figures 3 and 4 we made use of the EN4 analysis product of Good *et al.* (2013). EN.4.2.2 data were obtained from `https://www.metoffice.gov.uk/hadobs/en4/` and are ©British Crown Copyright, Met Office, provided under a Non-Commercial Government Licence.

Author ORCID. A. J. G. Nurser, https://orcid.org/0000-0001-8653-9258; S. M. Griffies, https://orcid.org/0000-0002-3711-236X; J. D. Zika, https://orcid.org/0000-0003-3462-3559; G. J. Stanley, https://orcid.org/0000-0003-4536-8602.

Appendix A. Example tracer subgrid operators

Our derivation of the subgrid scale tracer operator (6.8), which made use of exterior calculus, is distinct from those that commonly appear in the tensor analysis literature (e.g., Section 7.56 of Aris (1962) or section 21.5 of Griffies (2004)). The key distinction is that here we do not make use of a metric structure nor the corresponding covariant divergence operator. As illustration, we exhibit the subgrid operator using the sample $\boldsymbol{q}$-coordinates taken from Section 4.3 in which we assume the mapping $\mathfrak{q}$ from $\mathcal{X}$ to $\mathcal{Q}$ is bijective. We make use of the transformation (6.4) between the subgrid scale flux components written in $\boldsymbol{x}$-space and $\boldsymbol{q}$-space. For Cartesian coordinates with $\boldsymbol{q} = \boldsymbol{x}$ and $\mathfrak{m} = \rho$ we have

$$\rho\, \mathcal{D} = -\boldsymbol{\nabla} \cdot (\rho\, \boldsymbol{F}), \tag{A 1}$$

with $\boldsymbol{\nabla} = (\partial_x, \partial_y, \partial_z)$. For spherical coordinates, $q^\alpha = (\lambda, \phi, r)$, in which case $\mathfrak{m} = \rho\, r^2 \cos\phi$ and

$$F^\lambda = \boldsymbol{\nabla}\lambda \cdot \boldsymbol{F} = (r\cos\phi)^{-1}\, \hat{\boldsymbol{\lambda}} \cdot \boldsymbol{F} \tag{A 2a}$$

$$F^\phi = \boldsymbol{\nabla}\phi \cdot \boldsymbol{F} = r^{-1}\, \hat{\boldsymbol{\phi}} \cdot \boldsymbol{F} \tag{A 2b}$$

$$F^r = \boldsymbol{\nabla} r \cdot \boldsymbol{F} = \hat{\boldsymbol{r}} \cdot \boldsymbol{F}, \tag{A 2c}$$

with the spherical unit vectors written in terms of the Cartesian unit vectors

$$\hat{\boldsymbol{\lambda}} = -\hat{\boldsymbol{x}} \sin\lambda + \hat{\boldsymbol{y}} \cos\lambda \tag{A 3a}$$

$$\hat{\boldsymbol{\phi}} = -\hat{\boldsymbol{x}} \cos\lambda\, \sin\phi - \hat{\boldsymbol{y}} \sin\lambda\, \sin\phi + \hat{\boldsymbol{z}} \cos\phi \tag{A 3b}$$

$$\hat{\boldsymbol{r}} = \hat{\boldsymbol{x}}\, \cos\lambda\, \cos\phi + \hat{\boldsymbol{y}} \sin\lambda\, \cos\phi + \hat{\boldsymbol{z}} \sin\phi. \tag{A 3c}$$

The subgrid operator is thus given by

$$(\rho\, r^2\, \cos\phi)\, \mathcal{D} = -r\, \partial_\lambda\, (\rho\, \hat{\boldsymbol{\lambda}} \cdot \boldsymbol{F}) - r\, \partial_\phi\, (\rho \cos\phi\, \hat{\boldsymbol{\phi}} \cdot \boldsymbol{F}) - \cos\phi\, \partial_r\, (r^2\, \hat{\boldsymbol{r}} \cdot \boldsymbol{F}), \tag{A 4}$$

Finally, for generalized vertical coordinates, $q^\alpha = (x, y, \sigma)$, in which case $\mathfrak{m} = \rho\, (\partial z/\partial\sigma)$ so that

$$\rho\, (\partial z/\partial\sigma)\, \mathcal{D} = -\partial_\alpha [\rho\, (\partial z/\partial\sigma)\, F^\alpha], \tag{A 5}$$

with the generalized vertical coordinate representation of the flux given in terms of the Cartesian representation

$$F^x = \hat{\boldsymbol{x}} \cdot \boldsymbol{F} \quad \text{and} \quad F^y = \hat{\boldsymbol{y}} \cdot \boldsymbol{F} \quad \text{and} \quad F^\sigma = \boldsymbol{\nabla}\sigma \cdot \boldsymbol{F}. \tag{A 6}$$

Appendix B. Exterior forms, exterior algebra, and exterior calculus

In this appendix we provide a tutorial on *exterior forms*, which are also known as *differential forms*. Exterior forms are anti-symmetrized tensors that offer a rich, and physically useful, mathematical structure. They are central to the exterior algebra (also known as the Grassmann algebra) and the corresponding exterior calculus. We are concerned just with exterior forms in space, which conforms to a conventional study of classical mechanics where time is universal and thus has the same value regardless the chosen spatial coordinates, even if the spatial coordinates are time dependent. For simplicity, we use Cartesian coordinates. However, all results in this appendix hold regardless the coordinate choice, which is one of the key powers of exterior forms.

There is a rich literature in physics making use of exterior forms, with Flanders (1989) an early reference that features applications to thermodynamics, fluid mechanics, and Hamiltonian dynamics. Other treatments can be found in the general relativity text by Misner *et al.* (1973), the mathematical physics texts by Schutz (1980) and Frankel (2012), and the mathematics text by Fortney (2018). Warnick *et al.* (1997) and Warnick & Russer (2014) provide pedagogical treatments of electrodynamics using exterior forms, with their treatment of great use for our purposes. We also note that Cotter & Thuburn (2014) make use of exterior forms to derive novel numerical methods for the rotating shallow water equations.

Our discussion is terse and relatively superficial since we only require a small portion of the technology for this paper. Even so, we hope this appendix offers a useful entrée to the subject for the mathematically curious reader.

B.1. *Introducing exterior forms*

An exterior p-form is a covariant p-tensor that is anti-symmetric on all of its arguments. Sometimes we drop the "exterior" for brevity, thus referring just to p-forms. Although this definition may mean little to many readers, it turns out that exterior forms are actually quite familiar since they naturally appear inside of integrals. For example, a path integral along a curve, $\int_C (A\,\mathrm{d}x + B\,\mathrm{d}y + C\,\mathrm{d}z)$, in three dimensional space has an integrand defining an exterior 1-form

$$\mathfrak{A} \equiv A\,\mathrm{d}x + B\,\mathrm{d}y + C\,\mathrm{d}z, \tag{B 1}$$

where the smooth functions A, B, C are called the coefficients of $\mathfrak{A}$ and $\mathrm{d}x, \mathrm{d}y, \mathrm{d}z$ are differential increments of a Cartesian coordinate basis for three-dimensional Euclidean space. We say that equation (B 1) provides a Cartesian coordinate expression for the exterior 1-form $\mathfrak{A}$. Likewise, a surface integral, $\int_S [P\,\mathrm{d}y\,\mathrm{d}z + Q\,\mathrm{d}z\,\mathrm{d}x + R\,\mathrm{d}x\,\mathrm{d}y]$, leads to an exterior 2-form

$$\mathfrak{B} \equiv P\,\mathrm{d}y \wedge \mathrm{d}z + Q\,\mathrm{d}z \wedge \mathrm{d}x + R\,\mathrm{d}x \wedge \mathrm{d}y, \tag{B 2}$$

where $\wedge$ is the exterior (or wedge) product described below, with the exterior product carrying the anti-symmetry property of the 2-form. The volume integral, $\int_{\mathcal{V}} H\,\mathrm{d}x\,\mathrm{d}y\,\mathrm{d}z$, leads to an exterior 3-form

$$\mathfrak{C} \equiv H\,\mathrm{d}x \wedge \mathrm{d}y \wedge \mathrm{d}z. \tag{B 3}$$

Spaces with higher dimensions, $N > 3$, allow for higher order exterior forms. Note that the wedge product is associative, so that equation (B 3) is unambiguous.

B.2. *The exterior product and orientation*

Building anti-symmetry into the definition of p-forms renders information about orientation of geometric objects such as surfaces and volumes. Orientation is introduced into p-forms (with $p > 1$) through use of the exterior product, which is also known as the wedge product or Grassmann product. The exterior product of two 1-forms, φ and ζ, produces a 2-form by

defining the exterior product as the anti-symmetrized tensor (or outer) product

$$\varphi \wedge \zeta = \varphi \otimes \zeta - \zeta \otimes \varphi, \tag{B 4}$$

so that

$$\varphi \wedge \zeta = -\zeta \wedge \varphi \Longrightarrow \varphi \wedge \varphi = 0. \tag{B 5}$$

Note that we used anti-symmetry of the exterior product to put differentials of the 2-form (B 2) into right-handed cyclic order.

When placed inside of an integral, the area and volume element forms are defined by their familiar expressions from multi-variate calculus, yet with a sign (the orientation) carried by the exterior product according to a chosen "standard ordering". We choose 1, 2, 3 (i.e. x, y, z) to be the standard ordering. Hence, the oriented volume integral of an arbitrary function, Φ, is written

$$\int \Phi \, \mathrm{d}x \wedge \mathrm{d}y \wedge \mathrm{d}z = \int \Phi \, \mathrm{d}x \, \mathrm{d}y \, \mathrm{d}z = \int \Phi \, \mathrm{d}V, \tag{B 6}$$

whereas an odd permutation incurs a minus sign so that

$$-\int \Phi \, \mathrm{d}y \wedge \mathrm{d}x \wedge \mathrm{d}z = \int \Phi \, \mathrm{d}x \wedge \mathrm{d}y \wedge \mathrm{d}z = \int \Phi \, \mathrm{d}V. \tag{B 7}$$

In ordinary vector analysis we make use of a surface normal vector, such as $\hat{\boldsymbol{z}}$, to orient a surface in either the positive or negative $\hat{\boldsymbol{z}}$ directions. Anti-symmetry of the exterior product provides the exterior 2-form, $\mathrm{d}x \wedge \mathrm{d}y$, with the ability to both measure the area of the surface element and to orient the surface in space so that a normal vector is unnecessary. Thinking about the right hand rule, the exterior product incorporates the wrapping of the first and second fingers, and in so doing captures the orientation sense (clockwise or counter-clockwise). However, the exterior product jettisons the thumb since orientation only requires information within the surface and does not require information about directions outside the surface. We can thus conceive of the exterior product as enabling a thumb-less right hand rule.

The 3-form, $\mathrm{d}x \wedge \mathrm{d}y \wedge \mathrm{d}z$, is the oriented volume element for Euclidean three-space. A 3-form is the highest order exterior form available in three-dimensional space. The reason is that p-forms with $p > N$ all vanish due to anti-symmetry. It follows that all p-forms with $p = N$ are directly proportional to the volume form.

B.3. *The interior product*

The space of 1-forms is dual to the space of vectors. This relationship means that while vectors can be expressed, e.g., in terms of a Cartesian basis $\partial \boldsymbol{x}/\partial x^a$, a 1-form may be expressed in terms of the dual basis $\mathrm{d}x^a$, defined by $\mathrm{d}x^a(\partial \boldsymbol{x}/\partial x^b) = \delta^a_b$. The action of a (covariant) 1-form $\phi = \phi_a \mathrm{d}x^a$ on a (contravariant) vector $\boldsymbol{v} = v^a \partial \boldsymbol{x}/\partial x^a$ is then fully specified by linearity of ϕ, yielding the contraction

$$\phi(\boldsymbol{v}) = \phi_a v^a, \tag{B 8}$$

which is a scalar (0-form). Under these dual bases, the (covariant) 1-form $\phi_a \mathrm{d}x^a$ and the (contravariant) vector $\phi^a \partial \boldsymbol{x}/\partial x^a$ having the same component values are said to be *associated*.

The contraction in equation (B 8) can be generalised to the interior product, $i_{\mathbf{v}}\alpha$, which takes a p-form α to a $(p-1)$-form by contracting the vector, $\boldsymbol{v}$, with the first index of α. If the p-form is the exterior product of a q-form β and a $(p-q)$-form γ, the interior product is given by

$$i_{\mathbf{v}}(\beta \wedge \gamma) = [i_{\mathbf{v}}\beta] \wedge \gamma + (-1)^q \beta \wedge [i_{\mathbf{v}}\gamma]\,. \tag{B 9}$$

Where the p-form is built up as sequence of 1-forms, its interior product can be expanded by

(possibly repeated) application of (B 9). For instance

$$i_{\mathbf{v}}(A\mathrm{d}x \wedge \mathrm{d}y \wedge \mathrm{d}z) = [i_{\mathbf{v}}A\mathrm{d}x]\,\mathrm{d}y \wedge \mathrm{d}z - A\mathrm{d}x \wedge [i_{\mathbf{v}}(\mathrm{d}y \wedge \mathrm{d}z)]$$
$$= A\,(v^x \mathrm{d}y \wedge \mathrm{d}z + v^y \mathrm{d}z \wedge \mathrm{d}x + v^z \mathrm{d}x \wedge \mathrm{d}y). \tag{B 10}$$

B.4. *The exterior derivative*

The algebra of exterior forms is known as *exterior algebra*, whose properties largely follow from anti-symmetry of the exterior product. Likewise, the calculus of exterior forms is known as *exterior calculus*, whose properties are tied to the *exterior derivative* operator.

B.4.1. *Exterior derivatives*

The differential increment operator, d, is a fundamental part of Riemann integrals since it provides the infinitesimal increment needed to perform the integral. In the study of exterior forms, d is the exterior derivative, which is an anti-symmetrized differential operator that acts on a p-form and produces a $(p+1)$-form. Although the exterior derivative can be extended to both space and time coordinates, we are only concerned with the exterior derivative acting on the spatial coordinates, in which case

$$\mathrm{d} = \left[\mathrm{d}x\,\partial_x + \mathrm{d}y\,\partial_y + \mathrm{d}z\,\partial_z\right] \wedge . \tag{B 11}$$

When d is applied to a 0-form (a function), the exterior product reduces to standard scalar multiplication, so the exterior derivative takes the simpler form $\mathrm{d} = \mathrm{d}x^a \partial_a$. To apply d to a p-form (for $p \geqslant 1$), the coefficients of the p-form combine with the partial derivatives, whereas the differentials of the p-form combine (via the exterior product) with the differentials $\mathrm{d}x$, $\mathrm{d}y$, and $\mathrm{d}z$. Considering equation (B 11), the exterior derivative d is like a 1-form, but with partial derivatives for its coefficients.

The squared exterior derivative operator vanishes

$$\mathrm{d}\,\mathrm{d} = \mathrm{d}^2 = 0, \tag{B 12}$$

which is a key property we make use of in the following, and we illustrate it in Section B.4.7.

B.4.2. *Anti-symmetry of the exterior derivative*

Consider the exterior product of an arbitrary p-form, φ, and r-form, ζ. The exterior derivative of this exterior product is

$$\mathrm{d}(\varphi \wedge \zeta) = \mathrm{d}\varphi \wedge \zeta + (-1)^p \varphi \wedge \mathrm{d}\zeta, \tag{B 13}$$

thus reflecting the anti-symmetry properties of the exterior derivative when acting across the exterior product. Notably, the exterior derivative picks up the $(-1)^p$ factor as it crosses the p-form, φ, to then act on ζ.

B.4.3. *Exterior derivative of a 0-form*

The exterior derivative of a 0-form (a function) produces a 1-form

$$\mathrm{d}A = (\mathrm{d}x^a\,\partial_a)\,A = \mathrm{d}x\,\partial_x A + \mathrm{d}y\,\partial_y A + \mathrm{d}z\,\partial_z A. \tag{B 14}$$

B.4.4. *Exterior derivative of a 1-form*

The exterior derivative of a 1-form yields a 2-form. For example with $\mathfrak{A}$ from equation (B 1) we have

$$\mathrm{d}\mathfrak{A} = \mathrm{d}(A\,\mathrm{d}x) + \mathrm{d}(B\,\mathrm{d}y) + \mathrm{d}(C\,\mathrm{d}z) \tag{B 15a}$$
$$= \mathrm{d}A \wedge \mathrm{d}x + \mathrm{d}B \wedge \mathrm{d}y + \mathrm{d}C \wedge \mathrm{d}z \tag{B 15b}$$

where we dropped the d^2 terms due to the property (B 12). The final expression can be expanded by performing the exterior derivative on the functions A, B, C, thus yielding

$$\begin{aligned} \mathrm{d}\mathfrak{A} &= (\partial_y C - \partial_z B)\,\mathrm{d}y \wedge \mathrm{d}z \\ &\quad + (\partial_z A - \partial_x C)\,\mathrm{d}z \wedge \mathrm{d}x \\ &\quad + (\partial_x B - \partial_y A)\,\mathrm{d}x \wedge \mathrm{d}y. \end{aligned} \tag{B 16}$$

This result reveals the connection to the vector curl operation from 3D Cartesian vector analysis.

B.4.5. *Exterior derivative of a 2-form*

The exterior derivative of a 2-form is given by a 3-form. For example, with $\mathfrak{B}$ from equation (B 2) we have

$$\mathrm{d}\mathfrak{B} = \mathrm{d}(P\,\mathrm{d}y \wedge \mathrm{d}z) + \mathrm{d}(Q\,\mathrm{d}z \wedge \mathrm{d}x) + \mathrm{d}(R\,\mathrm{d}x \wedge \mathrm{d}y) \tag{B 17a}$$

$$= (\partial_x P + \partial_y Q + \partial_z R)\,\mathrm{d}x \wedge \mathrm{d}y \wedge \mathrm{d}z, \tag{B 17b}$$

which reveals the connection to the vector divergence operator from 3D Cartesian vector analysis.

B.4.6. *Exterior derivative of a 3-form*

The exterior derivative of a 3-form vanishes in three-dimensional space, which we see by

$$\mathrm{d}\mathfrak{C} = \mathrm{d}(H\,\mathrm{d}V) \tag{B 18a}$$

$$= (\partial_x H\,\mathrm{d}x + \partial_y H\,\mathrm{d}y + \partial_z H\,\mathrm{d}z) \wedge \mathrm{d}V \tag{B 18b}$$

$$= 0, \tag{B 18c}$$

where we wrote the volume 3-form as

$$\mathrm{d}V = \mathrm{d}x \wedge \mathrm{d}y \wedge \mathrm{d}z, \tag{B 19}$$

made use of the associativity property of the exterior product, and used anti-symmetry so that

$$\mathrm{d}x \wedge \mathrm{d}x = \mathrm{d}y \wedge \mathrm{d}y = \mathrm{d}z \wedge \mathrm{d}z = 0. \tag{B 20}$$

B.4.7. *Illustrating* $\mathrm{d}^2 = 0$

As illustrated here, the operator relation $\mathrm{d}^2 = 0$ (B 12) follows from the commutative property of mixed partial derivatives. Before starting, note that $\mathrm{d}^2 x = \mathrm{d}^2 y = \mathrm{d}^2 z = 0$, which we used in the examples above. These identities result from assuming constant differential increments for each coordinate. That is, as a function, $f(x) = x$ has a constant derivative and thus it has a zero second derivative.

Showing that $\mathrm{d}^2 A = 0$

The 1-form, $\mathrm{d}A$, from equation (B 14) has an exterior derivative given by

$$\mathrm{d}^2 A = \mathrm{d}(\partial_x A\,\mathrm{d}x + \partial_y A\,\mathrm{d}y + \partial_z A\,\mathrm{d}z). \tag{B 21}$$

Expanding the exterior derivative leads to

$$\begin{aligned} \mathrm{d}^2 A &= (\partial_{yx} A - \partial_{xy} A)\,\mathrm{d}x \wedge \mathrm{d}y \\ &\quad + (\partial_{zy} A - \partial_{yz} A)\,\mathrm{d}y \wedge \mathrm{d}z \\ &\quad + (\partial_{xz} A - \partial_{zx} A)\,\mathrm{d}z \wedge \mathrm{d}x \\ &\quad = 0, \end{aligned} \tag{B 22}$$

which follows from equivalence of the mixed partial derivatives.

Showing that $\mathrm{d}^2\mathfrak{A} = 0$

A few lines of algebra reveals that the 2-form, $\mathrm{d}\mathfrak{A}$, from equation (B 16), has a vanishing exterior derivative given by

$$\mathrm{d}^2\mathfrak{A} = 0, \tag{B 23}$$

which again follows from equality of mixed partial derivatives.

B.4.8. *Poincaré's Lemma*

Consider an arbitrary p-form, φ. We say the φ is closed if it has zero exterior derivative, $\mathrm{d}\varphi = 0$, whereas it is exact if it can be written as the exterior derivative of a $(p\text{-}1)$-form, $\varphi = \mathrm{d}\omega$. Since $\mathrm{d}^2 = 0$, an exact exterior form is also closed:

$$\varphi = \mathrm{d}\omega \implies \mathrm{d}\varphi = \mathrm{d}^2\omega = 0. \tag{B 24}$$

Poincaré's Lemma is a statement about the converse: all closed forms on simply connected manifolds are exact

$$\mathrm{d}\varphi = 0 \implies \varphi = \mathrm{d}\omega \tag{B 25}$$

for some ω. We made use of this theorem when introducing the $\boldsymbol{q}$-space streamfunction in Section 4.4.

Equation (B 24) generalizes a familiar result from three-dimensional vector analysis, namely that if a vector field $\boldsymbol{v}$ is conservative (it is the gradient of some scalar field f, so that $\boldsymbol{v} = \boldsymbol{\nabla} f$), then it is irrotational (it has zero curl, i.e. $\boldsymbol{\nabla} \times \boldsymbol{v} = \boldsymbol{\nabla} \times \boldsymbol{\nabla} f = 0$). Similarly, equation (B 25) generalizes the fact that $\boldsymbol{\nabla} \times \boldsymbol{v} = 0$ implies $\boldsymbol{v} = \boldsymbol{\nabla} f$ for some scalar field f, provided the domain is simply connected.

B.5. *Stokes-Cartan theorem*

The exterior calculus of exterior forms provides an elegant unification of the variety of integral theorems from vector calculus. We refer to the unified integral theorem as the *Stokes-Cartan theorem*, which is written

$$\int_{\mathcal{X}} \mathrm{d}\omega = \int_{\partial\mathcal{X}} \omega. \tag{B 26}$$

This relation holds for an exterior form, ω, of arbitrary order and thus for arbitrary dimensional spaces. Furthermore, the manifold $\mathcal{X}$ must be orientable and possess a smooth (or at least a piecewise smooth) boundary. For example, if the space is three-dimensional, then $\mathcal{X}$ is a volume and $\partial\mathcal{X}$ is the surface bounding the volume. If we are instead integrating over a two-dimensional space, then $\mathcal{X}$ is a 2-surface whereas $\partial\mathcal{X}$ is the one-dimensional curve bounding the surface. If we are integrating over a curve, then $\partial\mathcal{X}$ are the endpoints to the curve, in which case the Stokes-Cartan theorem reduces to the fundamental theorem of calculus. Finally, if $\mathcal{X}$ has no boundary, such as the surface of a sphere, then the right hand side of the Stokes-Cartan theorem (B 26) vanishes, and so too must the left hand side.

B.5.1. *The divergence theorem*

To connect equation (B 26) to the divergence theorem, let $\mathcal{X}$ be a closed volume in 3-space and let $\omega = \mathfrak{B}$, the 2-form given by equation (B 2), in which case $\mathrm{d}\omega$ is given by equation (B 17*b*). The Stokes-Cartan theorem (B 26) thus specializes to

$$\int_{\mathcal{X}} (\partial_x P + \partial_y Q + \partial_z R)\, \mathrm{d}x \wedge \mathrm{d}y \wedge \mathrm{d}z = \oint_{\partial\mathcal{X}} [P\, \mathrm{d}y \wedge \mathrm{d}z + Q\, \mathrm{d}z \wedge \mathrm{d}x + R\, \mathrm{d}x \wedge \mathrm{d}y]. \tag{B 27}$$

This equation is an expression of the divergence theorem, whereby the volume integral of the divergence of a vector field equals to the vector field integrated over the oriented area of

the surface bounding the volume. We emphasize the absence of a surface normal vector, as the exterior products are sufficient to orient the surface integrals.

B.5.2. *Vector calculus expression of Stokes' theorem*

Specializing ω to the 1-form $\omega = A\,\mathrm{d}x + B\,\mathrm{d}y + C\,\mathrm{d}z$ as in equation (B 1), so that $\mathrm{d}\omega$ is the 2-form in equation (B 16), and integrating over a 2-surface $\mathcal{A}$ with a one-dimensional boundary $\partial\mathcal{A}$ renders the Stokes-Cartan theorem (B 26) as

$$\int_{\mathcal{A}} [(\partial_y C - \partial_z B)\,\mathrm{d}y \wedge \mathrm{d}z + (\partial_z A - \partial_x C)\,\mathrm{d}z \wedge \mathrm{d}x + (\partial_x B - \partial_y A)\,\mathrm{d}x \wedge \mathrm{d}y] = \oint_{\partial\mathcal{A}} (A\,\mathrm{d}x + B\,\mathrm{d}y + C\,\mathrm{d}z), \quad \text{(B 28)}$$

where we assumed the right hand rule to orient the closed path integral. Equation (B 28) is the expression of Stokes' theorem commonly found in vector calculus treatments. On the horizontal plane, with $\mathrm{d}z = 0$, equation (B 28) reduces to *Green's theorem*.

REFERENCES

Aris, Rutherford 1962 *Vectors, Tensors and the Basic Equations of Fluid Mechanics*. New York: Dover Publishing.

Bi, Daohua, Dix, Martin, Marsland, Simon, O'Farrell, Siobhan, Sullivan, Arnold, Bodman, Roger, Law, Rachel, Harman, Ian, Srbinovsky, Jhan, Rashid, Harun A & others 2020 Configuration and spin-up of access-cm2, the new generation australian community climate and earth system simulator coupled model. *Journal of Southern Hemisphere Earth Systems Science* **70** (1), 225–251.

Cohen-Tannoudji, C., Diu, B. & Laloë, F. 1977 *Quantum Mechanics: Volume Two*. New York: John Wiley and Sons, 1524 + xxv pp.

Cotter, C. J. & Thuburn, J. 2014 A finite element exterior calculus framework for the rotating shallow-water equations. *Journal of Computational Physics* **257**, 1506–1526.

Davis, Russ E. 1994 Diapycnal mixing in the ocean: equations for large-scale budgets. *Journal of Physical Oceanography* **24**, 777–800.

Döös, K., Kjellson, J., Zika, J., Lalibertè, F., Brodeau, L. & Campino, A.A. 2017 The coupled ocean-atmosphere hydrothermohaline circulation. *Journal of Climate* **30**, 631–647.

Döös, K., Nilsson, J., Nycander, J., Brodeau, L. & Ballarotta, M. 2012 The World Ocean thermohaline circulation. *Journal of Physical Oceanography* **42**, 1445–1460.

Evans, Dafydd Gwyn, Zika, Jan D, Naveira Garabato, Alberto C & Nurser, AJ George 2014 The imprint of southern ocean overturning on seasonal water mass variability in d rake p assage. *Journal of Geophysical Research: Oceans* **119** (11), 7987–8010.

Evans, Dafydd Gwyn, Zika, Jan D, Naveira Garabato, Alberto C & Nurser, AJ George 2018 The cold transit of southern ocean upwelling. *Geophysical Research Letters* **45** (24), 13–386.

Flanders, H. 1989 *Differential Forms with Applications to the Physical Sciences*. New York: Dover Publications, 224 pp.

Fortney, J.P. 2018 *A Visual Introduction to Differential Forms and Calculus on Manifolds*. Switzerland: Springer Nature Switzerland, 468 pages.

Frankel, T. 2012 *The Geometry of Physics: An Introduction*. Cambridge University Press, 686.

Gill, A. 1982 *Atmosphere-Ocean Dynamics*, *International Geophysics Series*, vol. 30. London: Academic Press, 662 + xv pp.

Good, S.A., Martin, M.J. & Rayner, N. A. 2013 EN4: Quality controlled ocean temperature and salinity profiles and monthly objective analyses with uncertainty estimates. *Journal of Geophysical Research: Oceans* **118**, 6704–6716.

Gregg, M.C., D'Asaro, E.A., Riley, J.J. & Kunze, E. 2018 Mixing efficiency in the ocean. *Annual Reviews of Marine Science* **10**, 443–473.

Griffies, Stephen M. 1998 The Gent-McWilliams skew-flux. *Journal of Physical Oceanography* **28**, 831–841.

Griffies, Stephen M. 2004 *Fundamentals of Ocean Climate Models*. Princeton, USA: Princeton University Press, 518+xxxiv pages.

Griffies, S. M., Adcroft, A. & Hallberg, R. W. 2020 A primer on the vertical lagrangian-remap method in ocean models based on finite volume generalized vertical coordinates. *Journal of Advances in Modeling Earth Systems* **12**.

Groeskamp, S., Griffies, Stephen M., Iudicone, Daniele, Marsh, Robert, Nurser, A.J. George & Zika, Jan D. 2019 The water mass transformation framework for ocean physics and biogeochemistry. *Annual Review of Marine Science* **11**, 1–35.

Groeskamp, Sjoerd, Sloyan, Bernadette M, Zika, Jan D & McDougall, Trevor J 2017 Mixing inferred from an ocean climatology and surface fluxes. *Journal of Physical Oceanography* **47** (3), 667–687.

Groeskamp, S., Zika, J. D., McDougall, T. J., Sloyan, B. M. & Laliberté, F. 2014 The representation of ocean circulation and variability in thermodynamic coordinates. *Journal of Physical Oceanography* **44**, 1735–1750.

Hieronymus, Magnus, Nilsson, Johan & Nycander, Jonas 2014 Water mass transformation in salinity–temperature space. *Journal of Physical Oceanography* **44** (9), 2547–2568.

Holloway, Greg & Rhines, Peter B. 1991 Angular momenta of modeled ocean gyres. *Journal of Geophysical Research* **27**, 843–846.

Holmes, Ryan M., Zika, J.D. & England, Matthew H. 2019 Diathermal heat transport in a global ocean model. *Journal of Physical Oceanography* **49**, 141–161.

Iudicone, D., Madec, G. & McDougall, T. J. 2008 Water-mass transformations in a neutral density framework and the key role of light penetration. *Journal of Physical Oceanography* **38**, 1357–1376.

Kjellsson, Joakim, Döös, Kristofer, Laliberté, Frédéric B & Zika, Jan D 2014 The atmospheric general circulation in thermodynamical coordinates. *Journal of the Atmospheric Sciences* **71** (3), 916–928.

Laliberté, F., Zika, J. D., Mudryk, L., Kushner, P. J., Kjellsson, J. & Döös, K. 2015 Constrained work output of the moist atmospheric heat engine in a warming climate. *Science* **347**, 540–543.

Mackay, N., Wilson, C., Holliday, N. P. & Zika, J. D. 2020 The observation-based application of a regional thermohaline inverse method to diagnose the formation and transformation of water masses north of the OSNAP Array from 2013 to 2015. *Journal of Physical Oceanography* **50**, 1533–1555.

Mackay, N., Wilson, C., Zika, J. D. & Holliday, N. P. 2018 A regional thermohaline inverse method for estimating circulation and mixing in the Arctic and subpolar North Atlantic. *Journal of Atmospheric and Oceanic Technology* **35**, 2383–2403.

Marshall, John, Jamous, Daniel & Nilsson, Johann 1999 Reconciling thermodynamic and dynamic methods of computation of water-mass transformation rates. *Deep-Sea Research I* **46**, 545–572.

Misner, C. W., Thorne, K. S. & Wheeler, J. A. 1973 *Gravitation*. W.H. Freeman and Co., 1279 pages.

Nurser, A. J. George, Marsh, R. & Williams, R. G. 1999 Diagnosing water mass formation from air–sea fluxes and surface mixing. *Journal of Physical Oceanography* **29**, 1468–1487.

Olbers, D. J., Willebrand, J. & Eden, C. 2012 *Ocean Dynamics*, 1st edn. Berlin, Germany: Springer, 704 pages.

Pauluis, O. M. & Held, I. M. 2002 Entropy budget of an atmosphere in radiative-convective equilibrium. Part I: Maximum work and frictional dissipation. *Journal of the Atmospheric Sciences* **59**, 225–139.

Ruan, X. & Ferrari, R. 2021 Diagnosing diapycnal mixing from passive tracers. *Journal of Physical Oceanography* **51**, 757–767.

Salmon, Richard 1998 *Lectures on Geophysical Fluid Dynamics*. Oxford, England: Oxford University Press, 378 + xiii pp.

Salmon, R. 2013 An alternative view of generalized Lagrangian mean theory. *Journal of Fluid Mechanics* **719**, 165–182.

Schmitt, R. W. 1994 Double diffusion in oceanography. *Annual Review of Fluid Mechanics* **26**, 255–285.

Schutz, B. F. 1980 *Geometrical Methods of Mathematical Physics*. Cambridge, UK: Cambridge University Press, 250 pp.

Sohail, Taimoor, Zika, Jan D, Irving, Damien B & Church, John A 2022 Observed poleward freshwater transport since 1970. *Nature* **602** (7898), 617–622.

Speer, K. 1993 Conversion among North Atlantic surface water types. *Tellus* **45**, 72–79.

Speer, K. & Tziperman, E. 1992 Rates of water mass formation in the North Atlantic Ocean. *Journal of Physical Oceanography* **22**, 2444–2457.

Stakgold, I. 2000*a Boundary value problems of mathematical physics, volume I*. Philadelphia: SIAM, 340 pp.

Stakgold, I. 2000*b Boundary value problems of mathematical physics, volume II*. Philadelphia: SIAM, 408 pp.

Starr, V. P. 1945 A quasi-Lagrangian system of hydrodynamical equations. *Journal of Meteorology* **2**, 227–237.

Stommel, H. 1961 Thermohaline convection with two stable regimes of flow. *Tellus* **13**, 224–228.

van Sebille, E., Griffies, S.M., Abernathey, R., Adams, T.P., Berloff, P., Biastoch, A., Blanke, B., Chassignet, E.P., Cheng, Y., Cotter, C.J., Deleersnijder, E., Döös, K., Drake, H., Drijfhout, S., Gary, S.F., Heemink, A.W., Kjellsson, J., Koszalka, I.M., Lange, M., Lique, C., MacGilchrist, G.A., Marsh, R., Adame, G.C. Mayorga, McAdam, R., Nencioli, F., Paris, C.B., Piggott, M.D., Polton, J.A., Rühs, S., Shah, S.H., Thomas, M.D., Wang, J., Wolfram, P.J., Zanna, L., & Zika, J.D. 2018 Lagrangian ocean analysis: fundamentals and practices. *Ocean Modelling* **121**, 49–75.

Walin, Gösta 1977 A theoretical framework for the description of estuaries. *Tellus* **29** (2), 128–136.

Walin, G. 1982 On the relation between sea-surface heat flow and thermal circulation in the ocean. *Tellus* **34**, 187–195.

Warnick, K.F., Selfridge, R.H. & Arnold, D.V. 1997 Teaching electromagnetic field theory using differential forms. *IEEE Transactions on Education* **40**, 53–68.

Warnick, K. F. & Russer, P. 2014 Differential forms and electromagnetic field theory. *Progress In Electromagnetics Research* **148**, 83–112.

Weiss, J. B., Fox-Kemper, B., Mandal, D., Nelson, A. D. & Zia, R. K. P. 2019 Nonequilibrium oscillations, probability angular momentum, and the climate system. *Journal of Statistical Physics* **273–294**.

Winters, Kraig B. & D'Asaro, Eric A. 1996 Diascalar flux and the rate of fluid mixing. *Journal of Fluid Mechanics* **317**, 179–193.

Young, W. R. 2012 An exact thickness-weighted average formulation of the Boussinesq equations. *Journal of Physical Oceanography* **42**, 692–707.

Zika, J. D., England, M. H. & Sijp, W. P. 2012 The ocean circulation in thermohaline coordinates. *Journal of Physical Oceanography* **42**, 708–724.

Zika, J. D., Gregory, J. M., McDonagh, E. L., Marzocchi, A. & Clément, L. 2021 Recent water mass changes reveal mechanisms of ocean warming. *Journal of Climate* **34**, 3461–3479.

Zika, Jan D, Sijp, Willem P & England, Matthew H 2013 Vertical heat transport by ocean circulation and the role of mechanical and haline forcing. *Journal of physical oceanography* **43** (10), 2095–2112.